COMPUTATIONAL MODELING AND EXPERIMENTAL STUDY OF A WATER-BASED FREEZABLE HEAT EXCHANGER FOR USE IN HUMAN SPACECRAFT THERMAL CONTROL

by

JOSE MARIA MABRES ANTER

Advisor: Prof. James Nabity

Department of Aerospace Engineering Sciences

University of Colorado Boulder

July 2018

Acknowledgments

I want to thank my advisor James Nabity, all the Bioastronautics faculty members, and all the students of the Ann and H.J. Smead Aerospace Engineering Sciences that helped me to develop this work.

Additionally I would like to honor the efforts by BioServe Space Technologies for allowing me the use of their facilities.

Abstract

Mabres Anter, Jose M. (BS., Industrial Engineering, 2016; MS., Industrial Engineering,2018)

Computational Modeling and Experimental Study of a Water-Based Freezable Heat Exchanger for Use in Human Spacecraft Thermal Control

Thesis directed by Associate Professor James Nabity

A spacecraft thermal control system must keep the cabin and electronic equipment within operational temperature ranges by transporting heat out of the spacecraft. This process is generally accomplished with a series of heat exchangers. At the International Space Station, a water loop collects the heat loads and via a closed heat exchanger, this heat is transferred to an external anhydrous ammonia loop, where it circulates through large radiators located on the exterior of the Space Station, rejecting the heat by radiation to space.

A single loop instead of the actual dual-loop would simplify and reduce the complexity of the thermal control system. Besides, given the susceptibility of water to freeze and the toxicity of exposing the crew to ammonia it is hard to design a single-loop architecture.

A self-regulating freezable heat exchanger was designed in the past, to passively maintain and regulate thermal control through water ice buildup within the heat exchanger structure. In order to determine the feasibility and effectiveness of this technology, a computational model and experimental tests are needed. This is the main goal of this thesis work.

A computational model was developed with the ANSYS Fluent Software. The heat exchanger was simulated with different boundary conditions, and the influence of some parameters to the results was analyzed. A big focus of the analysis has been the study of the ice formation, and its wavy behavior.

Some experiments were made with the heat exchanger test apparatus, which was assembled again for this thesis work. Given the results of the simulation part, the experiments were oriented to understand the ice formation behavior. Some oscillations in the surface temperature measurements at the heat exchanger seem to confirm our hypothesis about the wavy behavior of the ice formation.

These results contribute to the growing body of work to develop and characterize freezable heat exchangers for spacecraft thermal control.

Contents

Nomenclature

Q	Heat Flux	$[W]$
h	Heat transfer coefficient	$[W/\mathrm{m}^2 \cdot \mathrm{K}]$
A	Heat transfer area	$[\mathrm{m}^2]$
ΔT	Temperature difference	$[\mathrm{K}]$
ε	Emissivity	
T	Temperature	$[\mathrm{K}]$
Re	Reynolds Number	
ρ	Density	$[kg/\mathrm{m}^3]$
v	Velocity	$[m/s]$
d	Tube Diameter	$[m]$
μ	Dynamic viscosity	$[Pa \cdot s]$
Cp	Specific heat	$[J/kg \cdot K]$
k	Thermal Conductivity	$[W/\mathrm{m} \cdot \mathrm{K}]$
θ	Freezing Parameter	

Chapter 1: Introduction

From the simplest satellite to the most complex human-rated vehicle, all spacecraft require thermal control. All spacecraft typically experience a wide range of heat loads during the course of a full orbit. For example, the International Space Station (ISS) in the sunlit (dayside) portion of the orbit, without thermal control, its temperature would ascend to 121°C (250°F) due to the energy transfer from the incident solar radiation combined with Earth's albedo and infrared (IR) energy, while the ISS in eclipse (nightside) will experience a cooler thermal environment, reaching temperatures of -157°C (-250°F), since the Earth eclipses the solar radiation from the spacecraft surface [1].

For protecting the spacecraft in both hot and thermal environments, multilayer insulation and thermal shields are used. But to keep the cabin comfortable the insulation is not enough, in fact, this insulation represents a significant challenge for thermal control. Unless heat is rejected to the surroundings, the internal temperature of the cabin will rise due to heat from avionics and other equipment.

Most of the Station's many systems produce waste heat, which needs to be transferred from the ISS to space to achieve thermal control and maintain components and the crew at acceptable temperatures. A Thermal Control System (TCS) is required to achieve this heat rejection function. The TCS uses a mechanically pumped fluid in closed-loop circuits to perform three functions: heat collection, heat transportation, and heat rejection. On the ISS, water coolant loops collect internal heat loads for transfer to an external anhydrous ammonia loop via an interface heat exchanger. The heated ammonia then circulates through large radiators located on the exterior of the Space Station, rejecting the heat by radiation to space that cools the ammonia as it flows through the radiators [1].

The ISS dual-loop thermal control architecture (water loops within the cabin and ammonia loops outside) requires sensors, active components and feedback control to ensure that the fluid temperatures remain within their allowable limits without freezing water. Further, toxic materials like ammonia impose constraints on design and require additional instruments to monitor for leaks. Together, these result in a complex architecture for spacecraft thermal control.

A single loop architecture employing phase change materials can offer numerous potential benefits to the TCS. A water-based cooling system would probably be the best option, but, as temperatures can be considerably below the freezing point of water, the volumetric expansion during freeze usually prevents its use in external systems since freezing will damage the components. Yet, if the system can accommodate the forces generated by freezing, then selectively allowing parts of a heat exchanger to freeze can be used to passively increase the turn-down of the heat rejection from radiators.

Phase change material (PCM) and flow-through freezable heat exchangers appear to be the most promising technologies to enable self-regulating spacecraft TCS with single loop architectures [2]. A PCM heat exchanger can provide temporary storage of the thermal energy on-board, and reject it during times when there is excess TCS capacity. This can save a substantial amount of mass and volume because the balance of the system can be designed to typical rather than worst case conditions. The NASA, UTC Aerospace Systems (UTAS), TDA Research, Inc. [3] and others have been developing and testing PCM heat sinks for spacecraft thermal control [2].

TDA Research, Inc. has been developing a freezable water/ice phase change heat exchanger (HXs) that will offer several advantages: they can eliminate the need for a separate heavy ammonia loop; use the buildup of ice to regulate the rate of heat transfer, and the endotherm of melting ice can absorb peak loads from the spacecraft to reduce the size and mass of the radiator.

This freezable water-based heat exchanger has been modeled, and has been tested experimentally. The robustness of the heat exchanger to both freeze and thaw without being damaged has been successfully verified. The heat exchanger hardware was physically tested and the test outputs were compared to the predicted results. While the entire range of input parameters were not analyzed, the preliminary analysis gave an indication that the freezable water-based heat exchanger was a feasible technology to reject heat from the spacecraft.

To prove that the heat exchanger technology is ready to enable the development of single loop architectures in a reduced-gravity environment, flight experiments are ultimately needed. Yet, computational modeling would help to test the feasibility of this technology more quickly and at lower cost than an experimental flight test with the hardware. However, a good computational model needs a broad range of experimental data for validation. To date, only a few conditions have been tested and always in steady state.

Therefore, the purpose of the following thesis is:

Characterize the performance of single loop architectures employing phase change materials for spacecraft thermal control.

This purpose will be assessed through the following tasks:

Computationally model and simulate water-based freezable heat exchangers to predict behavior and turndown in heat rejection for a range of spacecraft heat loads and environments.

Compare the results to experimental data and conduct additional experiments as needed to further validate the model.

Chapter 2: Background

In this following chapter, different concepts are explained in order to understand better the following thesis. As this thesis is focused on a freezable heat exchanger that uses water as a phase change material for spacecraft thermal control, it is important to understand the different forms of heat transport from first principles, know how the thermal control system of a spacecraft works, be able to describe the heat exchanger principle of operation, and be familiar with phase change materials. These concepts are discussed below and organized from the most general concept, to the most specific.

2.1. Heat Transfer

What is heat transfer? Or first, what is heat? As Incropera defines in the probably most famous heat transfer book *Fundamentals of Heat and Mass Transfer* [4], the energy can be transferred by interactions of a system with its surroundings. These interactions are called work and heat. The heat transfer is thermal energy in transit due to a spatial temperature difference. So that whenever a temperature difference exists in a medium or between media, heat transfer must occur.

We refer to different types of heat transfer processes as modes. When a temperature gradient exists in a stationary medium, which may be a solid or a fluid, we use the term conduction to refer to the heat transfer that will occur across the medium. In contrast, the term convection refers to heat transfer that will occur between a surface and a moving fluid when they are at different temperatures. The third mode of heat transfer is termed thermal radiation. All surfaces of finite temperature emit energy in the form of electromagnetic waves. Therefore, in the absence of an intervening medium, there is net heat transfer by radiation between two surfaces at different temperatures [4].

Modes of heat transfer

Conduction

Conduction is the transfer of heat from one part of a body at a higher temperature to another part of the same body at a lower temperature, or from one body at a higher temperature to another body in physical contact with it at a lower temperature. The conduction process takes place at the molecular level and involves the transfer of energy from the more energetic molecules to those with a lower energy level.

When evaluating conduction, the following equation is used to describe the heat flux:

$$Q = -k \cdot \nabla T \cdot A_s$$

In the equation, the minus sign is a consequence of the fact that heat is transferred in the direction of decreasing temperature. "Q" is the amount of energy transferred per unit time (in J/s, or W). The "k" term is a transport property known as the thermal conductivity and is a characteristic of the material, and is in units of W/(m·K). The "∇T" term is the temperature gradient across the two conducting materials (K/m). Lastly, the A_s term is used to describe the surface area (m^2) of the two materials in contact with one another.

As an example, the application of the conduction equation for a plane wall will provide us the next equation:

$$q = \frac{kA}{\Delta x}(T_2 - T_1)$$

As we can also see in Figure 1, Δx is the wall thickness, and T_1 and T_2 are the wall-face temperatures.

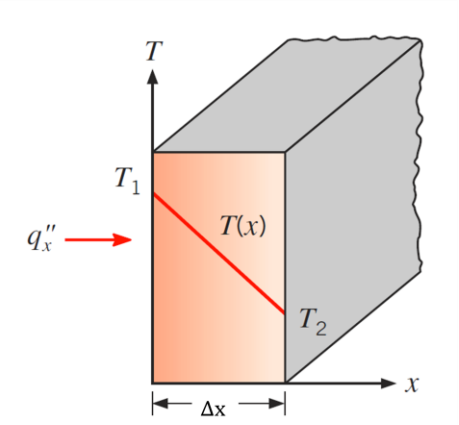

Figure 1 - One-dimensional heat conduction through a plane wall [4]

Convection

Convection relates to the transfer of heat from a bounding surface to a fluid in motion, or to the heat transfer across a flow plane within the interior of the flowing fluid. If the fluid motion is induced by a pump, a blower, a fan, or some similar device, the process is called forced convection. If the fluid motion occurs as a result of the density difference produced by the temperature difference, the process is called free or natural convection.

The following equation describes the heat transfer to an object through convection:

$$Q = -h \cdot A_s \cdot \Delta T$$

In the convection equation, "Q" is the heat flux (W). The "h" term is the convective heat transfer coefficient (W/m^2·K). The "A_s" term is the surface area of the object in contact with the fluid (m^2). The "ΔT" term is the difference in temperature between the object and the convective flow (K) [1].

Radiation

Radiation is the transfer of heat through electromagnetic waves traveling through space, emanating from a hot body exposed to a colder environmental sink. The following equation describes radiation from an object:

$$Q = \varepsilon \cdot \sigma \cdot A_{rad} \cdot T^4$$

In the radiation equation, "Q" is the heat flux (W). The "ε" term is the emissivity of the object radiating energy (unit less coefficient). The "σ" term is the Stefan-Boltzmann constant ($W/m^2 \cdot K^4$). The "A_{rad}" term is the surface area of the radiating body (m^2). The "T" term is the temperature of the radiating body (K). The radiation is actually a function of the difference between the radiating body and its surroundings. The radiator is assumed to be perfectly pointed towards deep space (0 K), with no obstruction or heat reflected back to the spacecraft which is why only one temperature term is used [1].

2.2. Fluid Dynamics

Fluid dynamics is the branch of physics that describes the motions of fluids. Fluids are divided into liquids and gases. In this present project, we are just going to focus in the study of one fluid, the water.

As it was explained before, the final goal of this thesis is to characterize the performance of a heat exchanger that will use water to control the temperature of a spacecraft. We are interested to see how water behaves in this heat exchanger, and how the properties or conditions of this fluid can affect the heat exchanger performance.

During this thesis, I use some concepts related to fluid dynamics that are very important for understanding the behavior of the heat exchanger, these concepts are explained below.

Laminar and turbulent flows

There are basically two different types of fluid motion, identified as laminar and turbulent flow. A very familiar example is shown in Figure 2. Here, whenever water is allowed to flow at a low velocity by opening the tap a little, the water flows out smoothly with its surface in the laminar state. But, as the tap is gradually opened to let the water velocity increase, fine-scale random fluctuations occur, and the flow becomes agitated and turbulent.

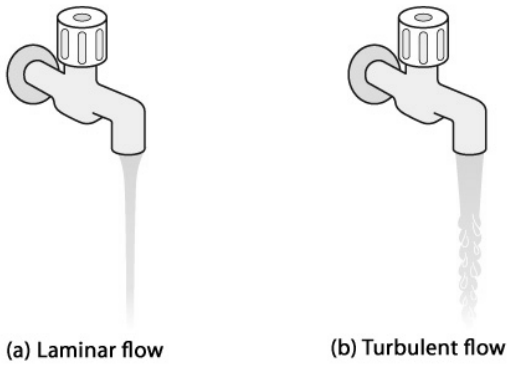

Figure 2 - Water flowing from a faucet [10]

A man named Osborne Reynolds studied such states of flow. He conducted many experiments and discovered that a laminar flow turns to a turbulent flow when the nondimensional quantity $\frac{\rho \cdot v \cdot d}{\mu}$ reaches a certain value that depends upon the average velocity v, glass tube diameter d, water density ρ and water viscosity μ.

This number from dimensional analysis is called the Reynolds number, and is calculated with the following equation:

$$Re = \frac{\rho \cdot v \cdot d}{\mu}$$

In circular pipes, a Reynolds number below 2300 is considered a laminar flow. For values between 2300 and 4000, the flow is called *transition flow*, and for values above 4000 is considered a turbulent flow.

In the following images, we see sketches of velocity distributions for laminar and turbulent flows over a flat plate (Figure 3) and in a pipe (Figure 4). The parabolic shape that we can see in the laminar case of Figure 4 follows a 2nd order polynomial profile, and the turbulent profile a 7th order polynomial.

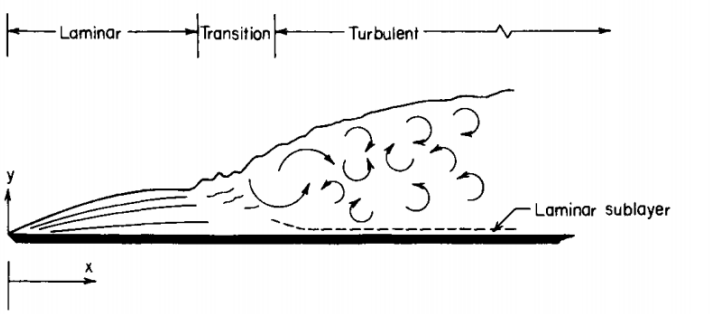

Figure 3 - Velocity distribution in a flat plate [10]

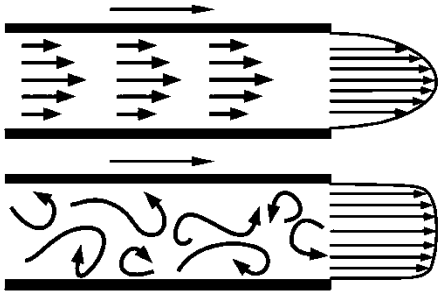

Figure 4 - Velocity distribution in a tube: laminar, turbulent [10]

This is important for my thesis because convective heat transport is substantially affected by the turbulence of the flow. Also, we will have to decide between different turbulence models in our computational design to correctly simulate the flow through a freezable heat exchanger.

Fluid properties

Density

It is the mass of the fluid per unit volume

Pressure

Pressure of a fluid is the force per unit area of the fluid. In other words, it is the ratio of force on a fluid to the area of the fluid held perpendicular to the direction of the force [26].

Temperature

It is the property that determines the degree of hotness or coldness, or the level of heat intensity of a fluid [26]. Temperature is measured by using temperature scales. There are three commonly used temperature scales:

- Fahrenheit scale
- Celsius (or centigrade) scale
- Kelvin scale (or absolute temperature scale)

Viscosity

Viscosity is the fluid property that determines the amount of resistance of the fluid to shear stress. It is the property of the fluid due to which the fluid offers resistance to flow [26]. Fluids with high viscosity deform slowly.

Specific heat (Cp)

Specific heat can be considered as the amount of energy required to increase the temperature of one unit of mass of a material by one degree.

Thermal conductivity

Thermal conductivity is the property of a material to conduct heat. Heat transfer occurs at a lower rate across materials of low thermal conductivity than across materials of high thermal conductivity. This property is temperature dependent and its reciprocal is thermal resistivity. [17]

Computational fluid dynamics

Computational fluid dynamics, commonly known as CFD, is a branch of fluid mechanics that uses numerical analysis and data structures to solve and analyze problems that involve fluid flows. Computers are used to perform the calculations required to simulate the interaction of liquids and gases with surfaces defined by boundary conditions.

The fundamental basis of almost all CFD problems is the Navier–Stokes equations, which define many single-phase fluid flows. The Navier-Stokes equations are the basic governing equations for a viscous, heat conducting fluid [32]. It is a vector equation obtained by applying Newton's Law of Motion to a fluid element and is also called the momentum equation. It is supplemented by the mass conservation equation, also called continuity equation and the energy equation.

Between the different CFD software to choose, for this project we selected ANSYS Fluent. Simulating a freezable heat exchanger is not easy, as we need to solve a liquid-solid multiphase flow, where there is a time-dependent moving interface between water and ice while conserving mass, momentum and energy. Conservation of mass in a freeze/thaw problem and conservation of energy in a fluid where melting and thawing will occur is a challenge for a CFD solver and for the modeler.

More detail about the methodology and the different methods used in ANSYS will be discussed in the simulation chapter.

2.3. Spacecraft thermal control

Controlling the level of temperature of equipment, payloads, satellites and launchers is essential during all phases of a space mission to protect flight hardware and to guarantee the optimum performance and success of a mission [13].

Thermal control maintains the spacecraft internal temperature within set parameters. For instance, a piece of equipment could, if encountering a temperature level which is too high, be damaged or its performance severely affected. In space it would hardly be possible to correct such a problem and this is why space thermal control systems need to be properly designed and tested and need to be very efficient and highly reliable. Thermal control is also what keeps the specified temperature stability for delicate electronics or optical components so as to ensure that they perform as efficiently as possible [13].

Therefore, in spacecraft design, the function of the thermal control system (TCS) is to keep the spacecraft's component systems within acceptable temperature ranges during all mission phases. It must cope with the external environment, which can widely vary as the spacecraft is exposed to deep space or to solar or planetary flux, and with rejecting to space the internal heat generated by the operation of the spacecraft itself [9].

The TCS comprises both passive and active components to maintain crew comfort and keep equipment within normal operating parameters. The TCS works in two ways:

- Protects the equipment from overheating, either by thermal insulation from external heat fluxes (such as the Sun or the planetary infrared and albedo flux), or by proper heat removal from internal sources (such as the heat emitted by the internal electronic equipment).

- Protects the equipment from temperatures that are too cold, by thermal insulation from external sinks, by enhanced heat absorption from external sources, or by heat release from internal sources

We differentiate between the passive and the active thermal control system. The purpose of the passive is the thermal protection, the purpose of the active, the thermal control.

The components used in the Passive Thermal Control System (PTCS) are insulation, surface coatings and heat pipes.

The Active Thermal Control System (ATCS) is responsible for collecting, transporting, and rejecting heat from the spacecraft. As the heat loads enter the spacecraft, the thermal energy is collected and transported to various locations. The incoming heat loads are absorbed by the heat exchangers, to be moved towards the heat sinks. The heat sinks reject the heat loads from the spacecraft [1].
The components and technology involved with the absorption, transfer, and rejection of heat are evaluated below.

Heat Absorption Components

When thermal radiation from low Earth orbit strikes a spacecraft, the incident energy can be absorbed, reflected, or transmitted through the spacecraft. In most cases, the spacecraft has reflective multilayer insulation (MLI) or coatings to reject incident solar energy and albedo from planetary surfaces and moons.
The spacecraft internal heat loads are absorbed by the heat exchangers or coldplates, to be moved by the heat transfer components towards the heat rejection components.

Heat Transfer Components

The heat transport from the absorption points towards the rejection points can be done with lots of different technologies, which are listed below [1]:

- Heat Transport Fluids
- Pumps
- Plumbing
- Heat pipes
- Heat straps

Heat Rejection Components

The rejection of the heat is usually done with:

- Radiators
- Evaporators
- Sublimators
- Phase change materials

    Used to store thermal energy during hot phases of cyclic thermal environments for later rejection during cold phases.

As an example, in the ISS the heat collection is done with five heat exchangers as well as cold plates, and the heat is ultimately rejected with radiators to deep space. But what happens between the heat collectors and the heat sinks? How is the heat transport done? Well, as explained in the introduction, my main goal of this thesis work was to assess feasibility for a single loop architecture using only water as the coolant for heat transport from equipment to the radiator.

ISS dual-loop thermal control architecture

As it was explained, a water loop collects heat generated within the spacecraft, and via a closed heat exchanger this heat is transferred to an external anhydrous ammonia loop, where it circulates through large radiators located on the exterior of the Space Station, rejecting the heat by radiation to space.

Figure 5 illustrates a simplified view of the dual-loop architecture used for ISS thermal management [2]. Water cooling loops also pick up heat from cold plates attached to the electronic equipment and experiments. To reject the heat, the inner water coolant flows through water/ammonia interface heat exchangers where the anhydrous ammonia loops then transport the heat to radiators, which in turn reject the heat to space [1]. Control of the amount of heat that flows from the ISS modules to the radiator is absolutely necessary, since the radiators are sized to handle the maximum heat load (75kW total), and will overcool the cabin if the heat transport rate cannot be controlled or the radiators regulated by reorientation.

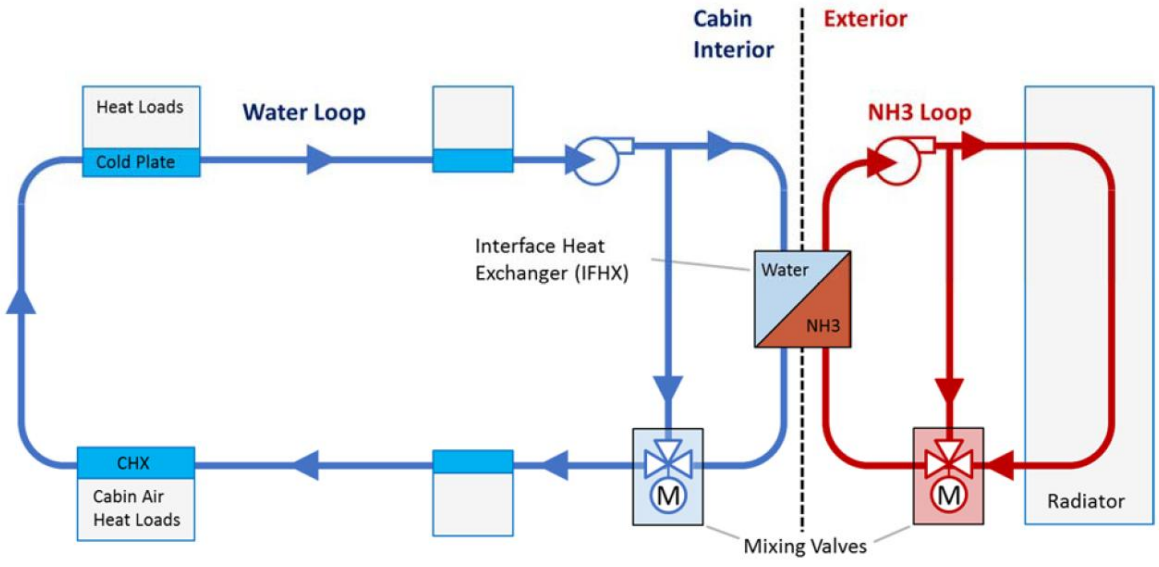

Figure 5 - The ISS dual-loop thermal control architecture, employing water loops within the cabin and ammonia loops outside the cabin [2]

For crew safety, the interface heat exchangers (IFHX) are mounted outside the ISS pressurized modules to minimize the risk of exposure to ammonia, a highly toxic compound. To keep water above its freeze point, the TCS uses an upstream mixing valve with bypass to keep the water within a narrow temperature range within the heat exchanger (between 3.3 and 5.5°C). Additional limits are in place to keep the ammonia coolant above the freeze point of water (2.8±1.1°C), which also helps to prevent water from freezing within the heat exchanger lines [2].

Single-loop thermal control architecture.

Given the susceptibility of water to freeze and the toxicity of exposing the crew to ammonia it's hard to design a single-loop architecture; besides, to achieve this will suppose a lot of benefits, and, in order to do it, we will need 1) to use non-toxic coolants that will not freeze during operation or 2) to employ freeze-tolerant heat exchangers and radiators. Both measures potentially allow relaxation of the control limits on fluid temperatures, can remove the ammonia cooling loop and thereby eliminate a toxic material while reducing system complexity, and can enable thermal management of space habitats with a single loop architecture [2]. For this thesis work we are focusing in the second measure: employ freeze-tolerant heat exchangers and radiators.

A single-loop, freezable cooling system has additional potential to simplify the TCS architecture: 1) freeze tolerant components will reduce the risk of structural damage posed by freeze, and 2) the selective freeze of the fluid loop can passively and autonomously increase the turndown of the heat rejection rate. The buildup and recession of a solid phase layer (e.g. ice) can modulate the heat flow to the radiators in proportion to the heat load from the space habitat and the external environment [2].

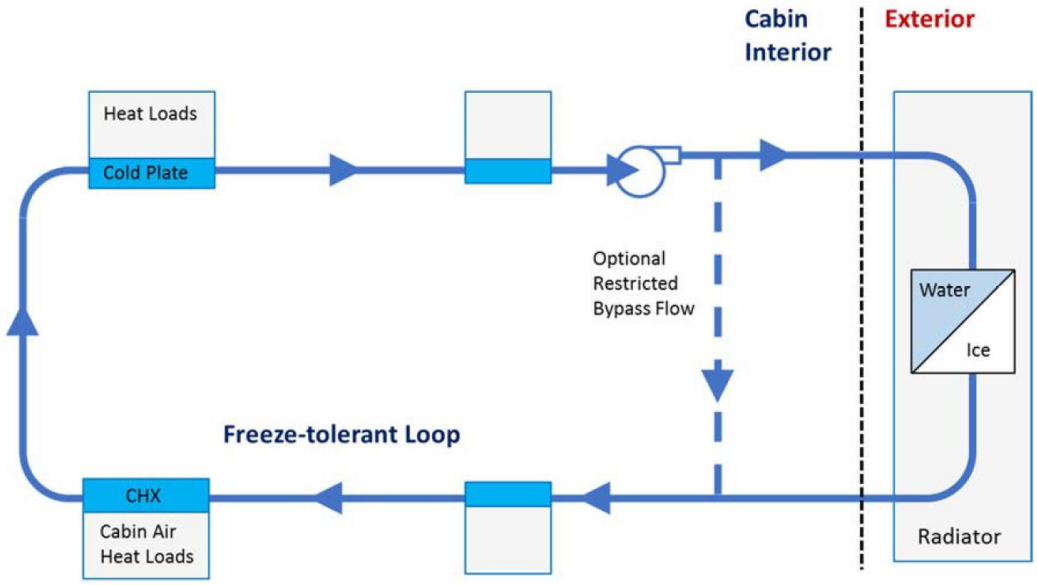

Figure 6 - A freezable, single-loop thermal control architecture [2].

2.4. Self-regulated heat exchanger (SRHX)

TDA Research, Inc. has been developing a freezable water/ice phase change heat exchanger. The main challenge was design of the heat exchanger taking into account that, as the outside temperatures of the spacecraft can reach very low values, the water will freeze, and this design must allow the water to freeze without blocking the pipe, and without breaking it due to the expansion of water when it changes from liquid to ice.

A robust freezable technology needs:

- Conductive structures with high surface area to transport heat from the cooling loop to radiators
- Provision for volumetric expansion and contraction of the coolant during phase changes
- A thermally isolated channel that flows coolant even when the surrounding structure is at temperatures below the coolants freeze point (the coolant will not freeze!)

Here I describe the freezable heat exchanger, technology that, if integrated into the radiator, could enable a single-loop architecture with potential for self-regulation of the thermal control. For this concept to work the heat exchanger must be able to freeze without structural failure, it must thaw quickly when the heat flux increases again, and the heat rejection capacity needs to respond in proportion to the load. In the laboratory unit (Figure 7), warm water flows through an inner tube and transfers heat to a refrigerated coolant that rejects heat to the environment. The inner tube has fins to help efficiently transfer heat to the wall (Figure 8); however, the space between two of the fins is insulated (from both the wall and the fins) so that the water flowing through that channel will stay above the freeze point even should the rest of the flow channels freeze solid.

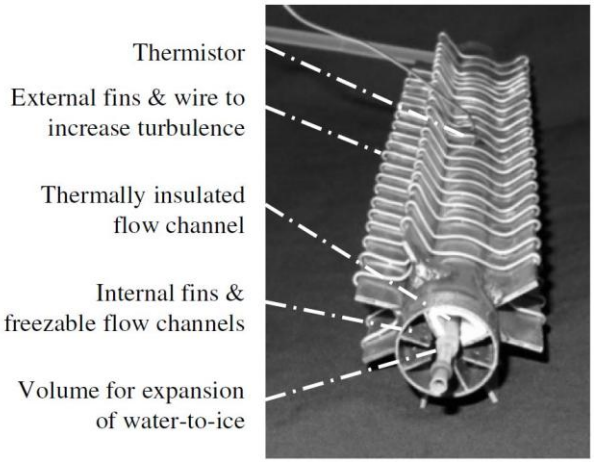

Figure 7 - Laboratory test unit [1]

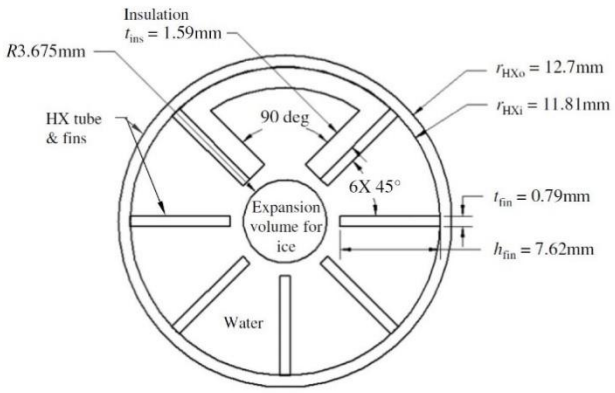

Figure 8 - Cross-sectional geometry [1]

In this thesis research, I want to computationally model this heat exchanger and simulate its behavior and reconstruct the test rig in order to conduct experiments at conditions needed to validate the model.

Chapter 3: Computational model. Freeze/thaw simulation and analysis.

In order to characterize the performance of the freezable heat exchanger, I would like to conduct several experiments with the test article under different situations. But experiments are expensive, in cost and time, and it is sometimes very hard to generate the needed boundary conditions (for example low temperatures of the tube's wall).

It is clear that we need a computational model to study our self-regulating heat exchanger (SRHX), in order to test it at different conditions. In addition, another goal of this model is to explore the influence of different parameters on heat exchanger performance and observe its behavior over a broad range of conditions.

The challenge of this part is to accurately simulate the SRHX, being able to verify the results with some experimental test, in order to know that the simulation is working well. And, the main challenge of this is to correctly simulate the ice formation, because CFD software solve single phase flows involving fluids and gases quite well, but they're not as good at modeling multiphase flows involving the formation of a solid phase. That is the reason why in this computational study one of the main objectives was to develop the methodology for using ANSYS Fluent to model this problem and then conduct simulations to observe how the formation of ice depends upon different parameters. The simulated behavior is then compared to experimental results.

My first step towards developing a model for the freezable heat exchanger was to first simulate pipe flow, and observe the freezing for different boundary and initial conditions. The goal here was to obtain results that could be compared to published experimental data.

R.R. Gilpin, in his paper *Ice Formation in a Pipe Containing Flows in the Transition and Turbulent Regimes* [8] studied ice nucleation of tap water in a pipe. Gilpin observed "…the development of a series of ice bands interspersed with ice-free zones" in other words, a thickening and thinning of the ice layer down the length of the pipe.

With the Gilpin paper we would compare our first models of ice formation in a single water pipe, after, with the correct modeling parameters concluded in the single pipe, we would simulate the SRHX.

As a summary, the main goal of this chapter is:

Computationally model and simulate water-based freezable heat exchangers to predict behavior and turndown in heat rejection for a range of spacecraft heat loads and environments.

The tasks in order to achieve this purpose will be the following:

- Simulate a single pipe flow: First without freezing to model the velocity profile and pressure loss for comparison with analytical calculations. Then, investigate the effect of ANSYS Fluent submodels, software parameters and material properties on computational stability and results.
- Model the pipe flow with freezing and compare to the Gilpin results. Select submodels and software parameters that are physically relevant, yet predict results most similar to those from Gilpin's experiments. We will need to decide:
    - General model
    - Turbulence model
    - Material properties
    - Boundary conditions
    - Calculation methods
- Compare the influence of different boundary conditions to the results.

- With the selected parameters, simulate the SRHX.

Freeze of water within a pipe was initially modeled in two CFD software: ANSYS Fluent and SolidWorks Flow Simulation. Of these, the ANSYS Fluent model was better grounded with physics-based models and more robustly produced results that made physical sense.

I have to say that not all these tasks were successful. Due to the limited computational capacity of available computers, I was not able to produce the same results as Gilpin experiments, and I had to focus the content of this chapter to model development to simulate freezing within a pipe through the study of the influence of the different submodels, model parameters and boundary and initial conditions. More work will be needed in the future to conduct converged mesh-independent simulations that will enable full validation of the model.

This chapter is organized following the tasks that have been just explained.

3.1. Freezing pipe flow

As I want to compare my freeze model with the Gilpin experiment, I will try to replicate his experiment computationally.

Geometry

I modeled the geometry used by Gilpin. The dimensions are the following:

		GILPIN MODEL	
GEOMETRY	Inner Diameter	0.033	meters
	Outer Diameter	0.035	meters
	Length	1.5	meters

At first, I designed the geometry and solved the problem in 3D, as the SRHX will be a 3D problem. However, the computers were slow to solve it in 3D with a lot of mesh elements, so I simplified the

problem to a 2D geometry. More specifically, as the geometry is circular, I solved the 2D axisymmetric problem needing only half of a 2D region illustrated in Figure 9.

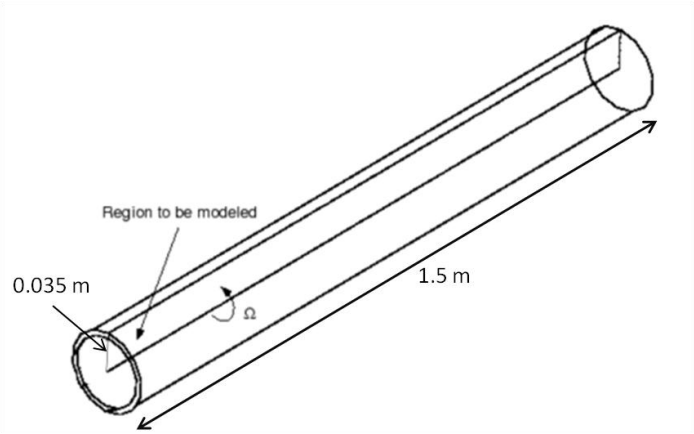

Figure 9 - Axisymmetric region to be modeled

Mesh

I began with a coarse mesh for the first trials with the intention to increase the elements to get mesh independent solutions with the set of parameters that correctly model freezing pipe flow. In order to create a refined mesh near the wall, I used the option for inflation layer meshing. Figure 10 shows the resulting mesh of my 2D model.

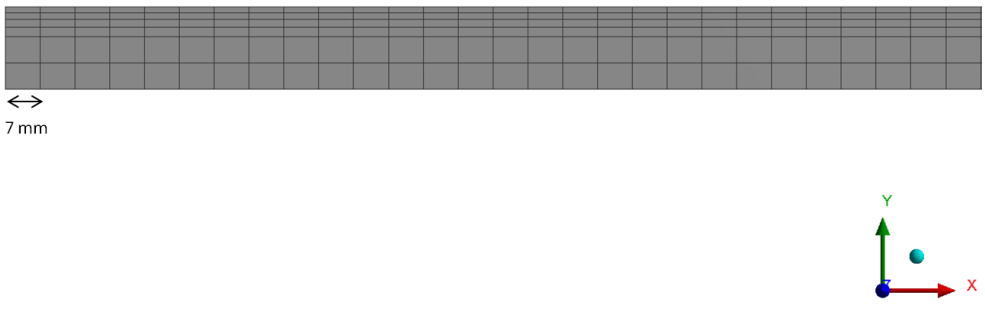

Figure 10 - Left end of the meshing of the 2D axisymmetric model

Set up

For modeling this problem in ANSYS Fluent, the following aspects must be set:

General - Solver

Type: pressure-based

Velocity formulation: absolute

2D Space: Axisymmetric

Time: Both steady and time-accurate solutions were obtained. Although the time-accurate simulation implies a longer time for the calculation, it was the option mostly used since it gave the more robust and stable solutions.

Gravity: I solved the problem both with and without gravity, observing that the results did not change by much.

Models

For solving this problem, we need the calculation of the energy and heat transfer, so we must enable the energy model.

In order to solve for freeze and thaw, I neeeded to employ a multiphase model. I selected the solidification/melting model within ANSYS Fluent rather than the multiphase model. The explanation of this method, regarding to the ANSYS manual is the following:

> *FLUENT can be used to solve fluid flow problems involving solidification and/or melting taking place at one temperature (e.g., in pure metals) or over a range of temperatures (e.g., in binary alloys). Instead of tracking the liquid-solid front explicitly, FLUENT uses an enthalpy-porosity formulation. The liquid-solid mushy zone is treated as a porous zone*

with porosity equal to the liquid fraction, and appropriate momentum sink terms are added to the momentum equations to account for the pressure drop caused by the presence of solid material. Sinks are also added to the turbulence equations to account for reduced porosity in the solid regions. FLUENT provides the following capabilities for modeling solidification and melting:

• Calculation of liquid-solid solidification/melting in pure metals as well as in binary alloys

• Modeling of continuous casting processes (i.e., "pulling" of solid material out of the domain)

• Modeling of the thermal contact resistance between solidified material and walls (e.g., due to the presence of an air gap)

• Postprocessing of quantities related to solidification/melting (i.e., liquid fraction and pull velocities) These modeling capabilities allow FLUENT to simulate a wide range of solidification/melting problems, including melting, freezing, crystal growth, and continuous casting. The physical equations used for these calculations and the instructions for setting up and solving a solidification/melting problem are provided in the manual [19].

One important limitation of this model is that one cannot specify material properties separately for the solid and liquid materials. That means that a single material must be created with the correct properties, defined as a function of temperature, for both the liquid and solid phases.

The other model that we need to choose is the viscous model. ANSYS uses different equations to solve laminar and turbulent flows. Since there can be either flow regime within the SRHX, I chose the model most appropriate for each problem based on the flow Reynolds number.

However, choosing the turbulence model was not easy, because the flow will change its turbulence due to the buildup of ice along the walls, which blocks the passage of the liquid and will change the flow conditions. Also, from Gilpin's experiments we know that the formation of ice waves will also affect the flow conditions down the length of the pipe. As he says: "…in the converging flow-passage on the upstream of each ice-band the flow acceleration appears to be strong enough to relaminarize the flow."

That means that even for a turbulent flow we may have some laminar zones, and so I have the challenge that the flow can be laminar at some time and location and turbulent at others coupled with the problem that the turbulence models do not simulate well the laminar flow (and the laminar model does not simulate well a turbulent flow).

The different models were tried and analyzed, and finally the decision was the following:

For flows with a very low Reynolds I will use the laminar model, because even if the turbulence of the flow changes, I still expect laminar flow. For flows with transient Reynolds numbers or high Reynolds numbers I will use the standard k-omega (2 equation) turbulence model, with the feature of Low-Re corrections. I also considered the k-epsilon model that gave very similar results, but the k-epsilon model does not have the Low-Re feature.

Regarding to the standard k-omega turbulence model, the turbulence kinetic energy, k, and the specific dissipation rate, ω, are obtained from the following transport equations [11]:

$$\frac{\partial}{\partial t}(\rho k) + \frac{\partial}{\partial x_i}(\rho k u_i) = \frac{\partial}{\partial x_j}\left(\Gamma_k \frac{\partial k}{\partial x_j}\right) + G_k - Y_k + S_k$$

$$\frac{\partial}{\partial t}(\rho\omega) + \frac{\partial}{\partial x_i}(\rho\omega u_i) = \frac{\partial}{\partial x_j}\left(\Gamma_\omega \frac{\partial \omega}{\partial x_j}\right) + G_\omega - Y_\omega + S_\omega$$

In these equations, G_k represents the generation of turbulence kinetic energy due to mean velocity gradients. G_ω represents the generation of ω. Γ_k and Γ_ω represent the effective diffusivity of k and ω, respectively. Y_k and Y_ω represent the dissipation of k and ω due to turbulence. All of the above terms are calculated as described below. S_k and S_ω are user-defined source terms [11].

The Low Reynolds correction feature is very important to obtain a reliable model. We will need it due to our flow conditions, which will have some areas with different flow turbulence, due to the ice band behavior already explained. The relaminarization of the flow at the ice bands will decrease the Reynolds number at the end of the contraction of an ice band.

The most widely-used engineering turbulence model for industrial applications is the k-epsilon, but the k-omega family of turbulence models have gained popularity mainly because:

- The model equations do not contain terms that are undefined at the wall, i.e. they can be integrated to the wall without using wall functions. (we need wall functions for the k-epsilon model).
- They are accurate and robust for a wide range of boundary layer flows with pressure gradient.

The standard k-omega uses a two-transport-equation model solving for k and ω, the specific dissipation rate (ε / k) based on Wilcox (1998). It demonstrates superior performance for wall-bounded and low Reynolds number flows, has potential for predicting transition, and has options to account for transitional, free shear, and compressible flows.

In addition, I wanted to be sure that the model was simulated correctly, so as previously stated, I first modeled pipe flow without freezing to verify that the model produced the expected velocity profile and pressure loss. Pipe flow was modeled with the wall temperature above the freezing point of water. The

resulting velocity profile and the pressure loss were analyzed. I compared the pressure loss from the simulation with a simple calculation of Hagen–Poiseuille pressure loss in a pipe.

$$\Delta P = \frac{8\mu \mathrm{LQ}}{\pi R^4}$$

I wanted to do this especially to verify that the k-omega with Low Reynolds corrections was able to model well a laminar flow. For the case I simulated, the pressure loss obtained analytically with Hagen–Poiseuille was ΔP = 0.108 Pa, and from the ANSYS simulation ΔP = 0.109 Pa. The velocity profile obtained appears appropriate for a laminar flow (compare Figure 11 to Figure 4).

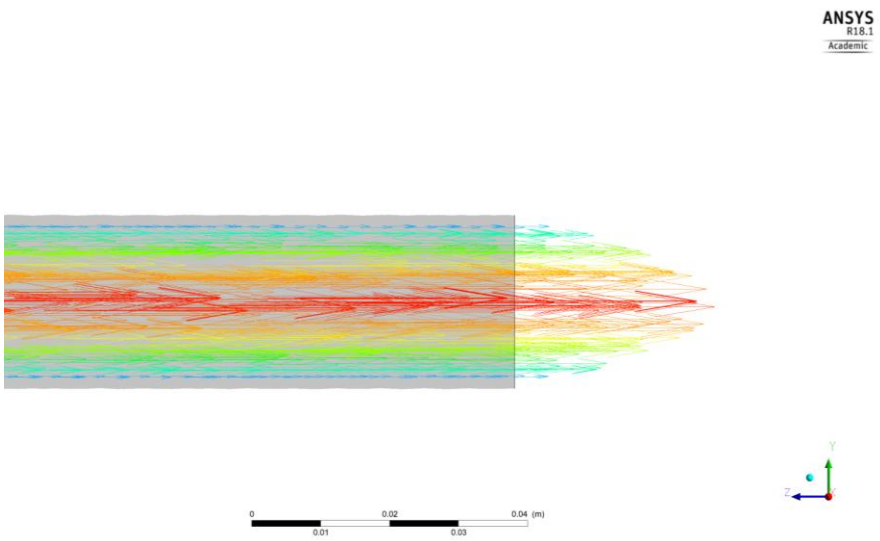

Figure 11 – Velocity profile single pipe flow without freezing

Materials

Unlike the multiphase model, the simulation/melting model cannot specify material properties separately for the different phases of a material. Therefore, instead of selecting the materials water-liquid and water-solid available within Fluent, I created a new material with the properties of both states of the material as a function of the temperature.

In the trials with the Solidworks Flow Simulation CFD software, as this code does not have neither a simulation/melting model nor a multiphase model, I created a single material by modifying the database for water to incorporate the effects of freezing. At 0°C the viscosity was increased by several orders of magnitude to simulate a solid. The heat of fusion was accounted for by modifying the specific heat (Cp) over a very small temperature difference at the freeze point. These modifications did not work as well as the ANSYS solidification/melting model, where I just needed to introduce the properties, the solid/melting temperature and the latent heat, without need to modify the properties to simulate the phase change. A physics-based model to conserve energy accounted for the latent heat of fusion.

The material properties were defined for density, specific heat, thermal conductivity and viscosity. Although the density changes in function of the temperature and between different phases, for this work, constant densities in both melt and solid regions were assumed; necessary to obtain converged results. The behavior of ANSYS with variable density was not satisfactory.

For the other physical properties, I was able to introduce the dependence on temperature. There is much data for each property from relevant literature, however I used a reduced set of nine values to define each property as a function of temperature. In the following figures, I present a graph and comments for each property. As you will see, the data are more closely spaced for the range of temperatures important to the simulation, and fewer points were used outside this range.

Dynamic Viscosity

In its liquid state, the water viscosity decreases as we increase the temperature. In its solid phase, the water will be treated as a solid, ice. We can see the values introduced to the program in the following Figure 12.

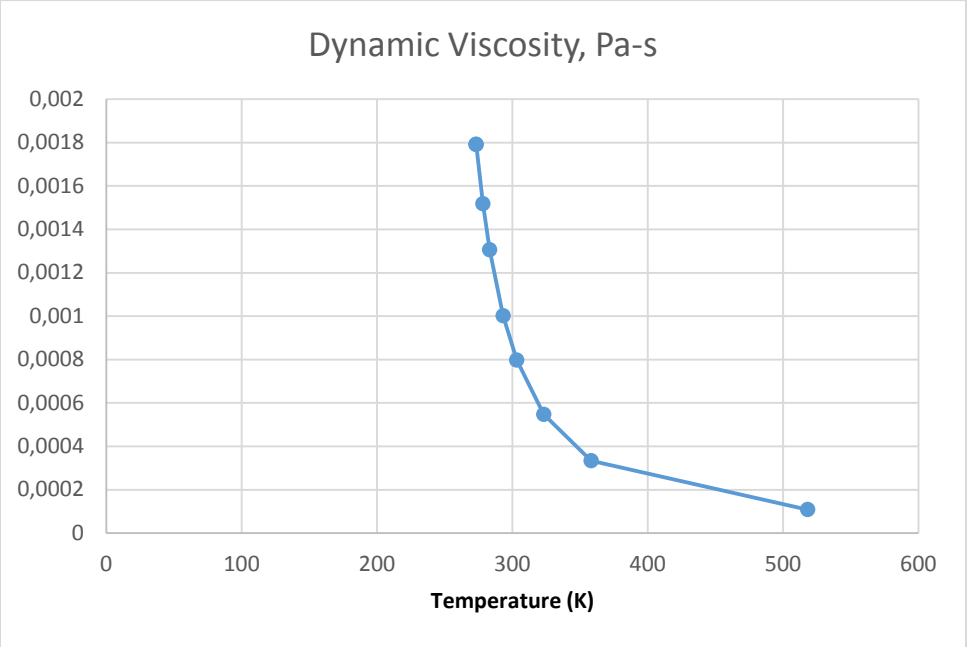

Figure 12 – Dynamic viscosity of the water

Specific Heat

The specific heat of water in its solid state is lower than in its liquid state. Also, in its liquid state the specific heat is variable in function of temperature. We can see the values introduced to the program in the following Figure 13.

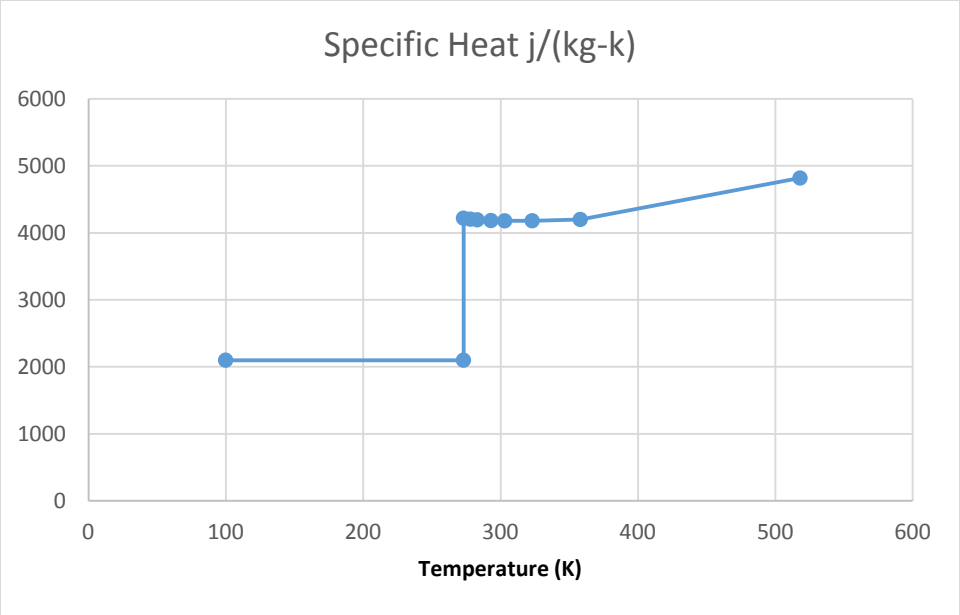

Figure 13 – Specific Heat of water

Thermal conductivity

The thermal conductivity of water in its solid state is higher than in its liquid state. Also, the liquid water changes its thermal conductivity in function of its temperature. We can see the values introduced to the program in the following Figure 14.

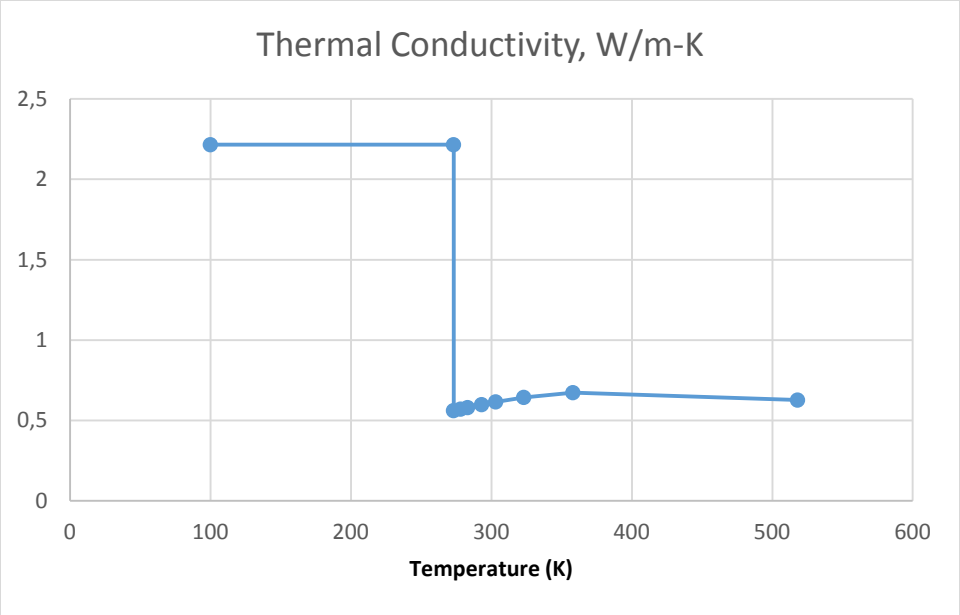

Figure 14 – Thermal conductivity of water

The other material that we have to introduce to the software is our solid material, the material of our tube. We introduced the properties of the aluminum A16061-T6, the one that we used for our experimental test. (Density of 2719 kg/m3, Specific Heat of 971 J/kg-K, and a thermal conductivity of 202.4 W/m-K)

Boundary conditions

For simulating our model, we need to simulate three important zones:

- Water inlet
    - Water is introduced at a certain temperature and with a constant mass flow, which will lead to a flow with a specific Reynolds number.
- Water outlet
    - The water condition is a pressure-outlet condition.
- Wall

- There are many ways to simulate the heat transfer between the inside of the heat exchanger and the outside. For example, I could simulate it as a heat flux on the wall, or as a constant temperature at the wall. It was modeled with a constant temperature at the outer wall, since this boundary condition most closely approximates the experiment.

These three areas lead us to four boundary conditions to introduce:

1. Water inlet temperature
2. Water inlet mass flow
3. Water outlet pressure
4. Outer wall temperature

For the boundary temperatures, I first needed to define the freezing parameter θ, used in Gilpin's experiment. His experimental apparatus consisted of two concentric glass tube surrounded by a square acrylic box. The water in which freezing occurred was pumped through the center tube. The coolant (methanol and water) was circulated at high velocity through a 3 mm wide annulus between the two tubes. The outer box was filled with an ethylene glycol-water mixture and was intended to minimize the optical distortion caused by the curved walls of the glass pipes. The combination of the different temperatures used in the experiment defined the freezing parameter, θ. The equation is the following:

$$\theta = \frac{T_f - T_c}{T_w - T_f}$$

Where T_f is the temperature of the freezing point, T_c is the coolant temperature, and T_w is the water inlet temperature.

As we know that Gilpin used a freezing parameter of 13.3, I could obtain from its equation the different combinations of values for the water inlet and the wall temperatures. From the different options, I chose a water inlet temperature of 275 K, and a constant wall temperature of 248.5 K.

The mass flow will depend on the desired level of turbulence. For the SRHX I will model with the same mass flow used in the experiments. In this case, as I am interested to compare my results with Gilpin experiments, I will try to replicate his flow. In his paper, one can see images of the freezing in two fluid situations, one with a Reynolds number of 3,025 and the other with 13,500. Afterwards, in order to expand my study, I added two cases: one laminar flow and one more turbulent with Reynolds numbers of 1,200 and 36,000, respectively.

To calculate the mass flow I used the Reynolds equation for single pipe flows:

$$Re = \frac{\rho \cdot v \cdot D}{\mu}$$

Where ρ is the density, v is the velocity, D the diameter and μ the dynamic viscosity. With this equation, we can know the velocities, and after we can calculate the mass flow. For our four Reynolds numbers, we obtained the following mass flows:

Re 1200	0.054 kg/s
Re 3025	0.137 kg/s
Re 13500	0.609 kg/s
Re 36000	1.625 kg/s

Table 1 - Mass flows used in the CFD simulation

The water outlet pressure will be constant for all cases, modeled to be a 0 Pascal outlet (gauge pressure) equivalent to a water outlet open to the atmosphere.

All these four conditions explained (water inlet temperature, water inlet mass flow, water outlet pressure and outer wall temperature) were selected in order to replicate Gilpin's experiment as best as possible.

Numerical method

The governing equations with wall boundary conditions, and inlet and outlet boundary conditions were solved in a Cartesian coordinate system by the ANSYS Fluent CFD solver using a finite volume method. The second order upwind implicit scheme with a segregated solver was selected to solve the continuity, momentum and energy equations solved, and the PISO algorithm was used for the pressure-velocity coupling. To avoid the divergence, the under-relaxation technique was applied to all dependent variables. In the investigation, the under-relation factor for the pressure was 0.1-0.3, that for the velocity components was 0.1–0.3, and those for the turbulence kinetic energy and turbulence dissipation rate were 0.3–0.5.

After setting the numerical method and before running the solver, we must initialize the calculation and choose some calculation parameters. When we initialize the calculation, it is important to patch the initial value of the water temperature, we want to have the initial value of fluid temperature at the same temperature as the inlet, at 275°K; for the other parameters, we chose the default values.

The most important calculation parameter for transient simulations was the time step, which influences the solution convergence stability and accuracy. A small time step will demand a very long time for solving the problem, but will result in better convergence and accurate results. With a large time step, the simulation will run faster, but the solution may diverge. Even with convergence, we may obtain wrong results. After calculating the largest time step possible for accurate results (using a stability

equation as a function of velocity and of the length of the Δx divisions of the mesh), I chose a 0.01s time step. Small enough for convergence stability and large enough to reach some hours of simulation time for observation of the Gilpin ice band phenomena. However, when I wanted just to observe the ice growth of the first minutes in the pipe, I sacrificed computational cost in order to get better accuracy with a time step of 0.001s. This would normally incur much time for solving the problem, but the computational time was reasonable since I only needed minutes of simulation time. Yet, it still took almost 24 hours to simulate just 1 minute of the freezing flow.

Results

I simulated the different flows to predict ice growth, and temperature, pressure and velocity fields. The most interesting data and graphics are shown below.

First, it is interesting to see, for each case, how the mass-averaged temperature and liquid fraction drop with time. We can see it in the next graphics.

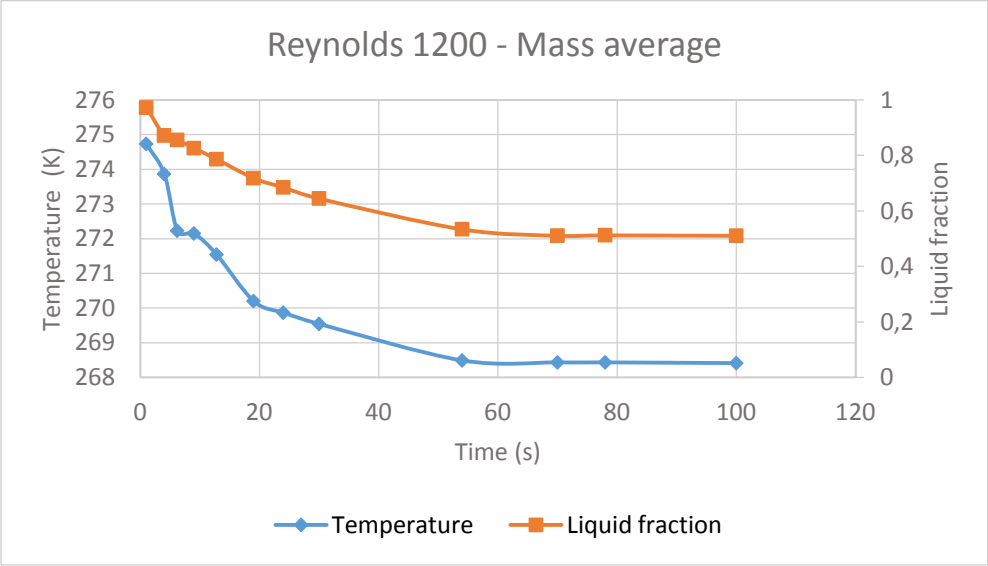

Figure 15 – Mass-average temperature and liquid fraction for a 1200 Reynolds flow.

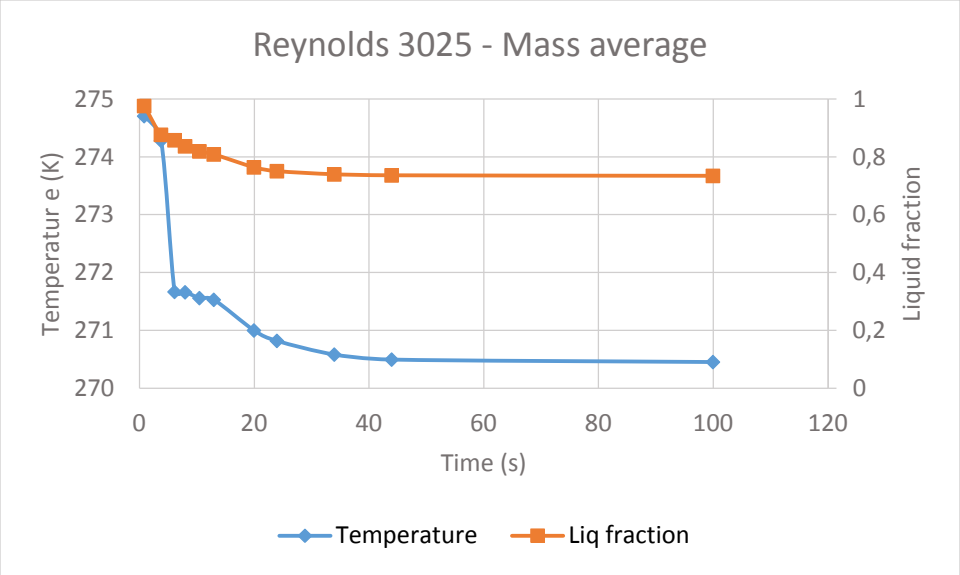

Figure 16 – Mass-average temperature and liquid fraction for a 3025 Reynolds flow

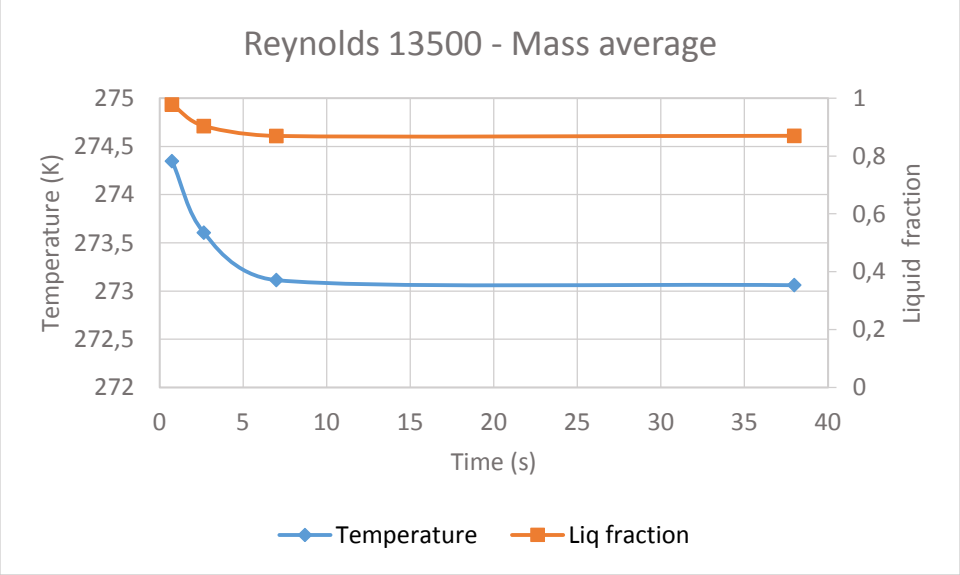

Figure 17 – Mass-average temperature and liquid fraction for a 13500 Reynolds flow

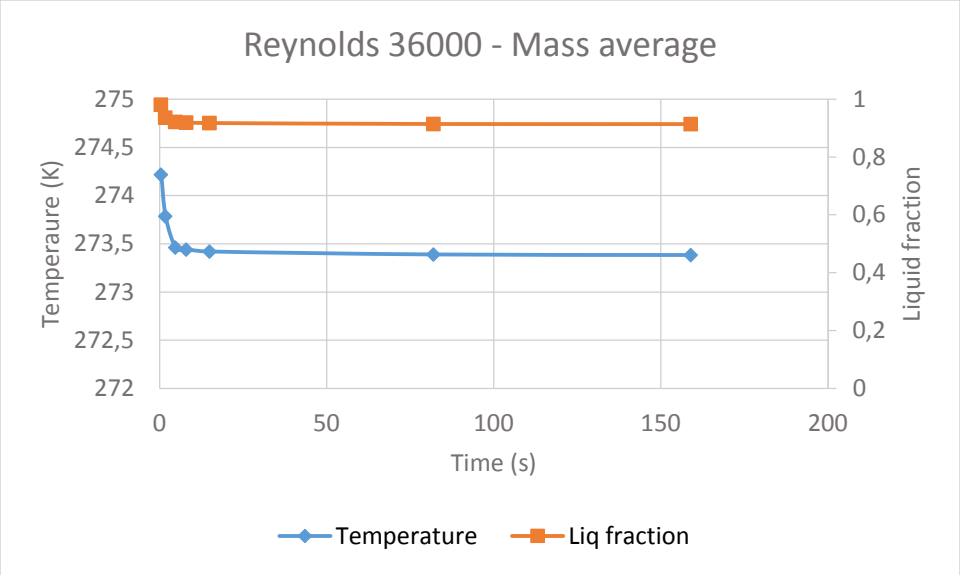

Figure 18 – Mass-average temperature and liquid fraction for a 36000 Reynolds flow

As expected, the higher the mass flow, the higher the mass-averaged temperatures and liquid fractions. For all cases, a steady state was reached without freezing completely the pipe. For flows with Reynolds numbers approximately less than 1,000, the liquid fraction nearly dropped to 0 indicating that the pipe was almost filled with ice. In that case, the solid phase reached the centerline axis of the pipe. The following Figure 19 shows the ice thickness for the different cases. Using this graph, one can predict the ice thickness as a function of the Reynolds number.

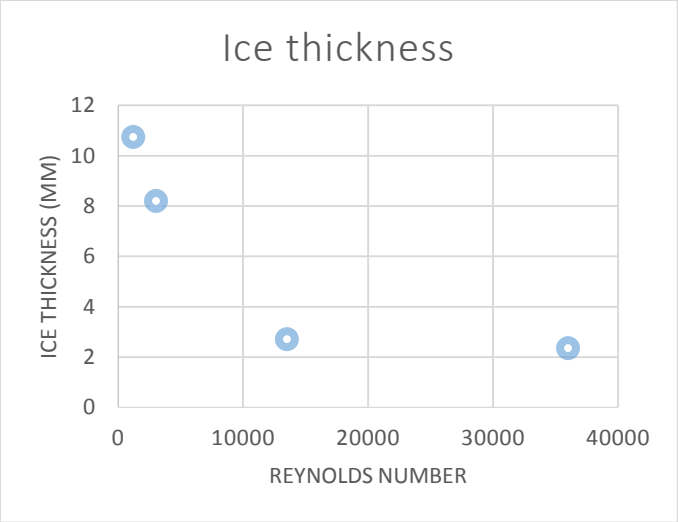

Figure 19 - Ice thickness (mm) in function of Reynolds number

When the solid phase is forming, the open transversal area reduces and, therefore, the effective area of the pipe becomes smaller and smaller, due to the increasing thickness of the solid layer.

During the solidification process in a pipe, the interface between liquid and solid regions moves from the pipe wall toward the centerline. The surface heat flux reduces due to increased thermal resistance of the solid zone stemming from the thickened layer of ice.

The ice blockage of each case can be calculated from the liquid fraction at the outlet in its steady state (Figure 20).

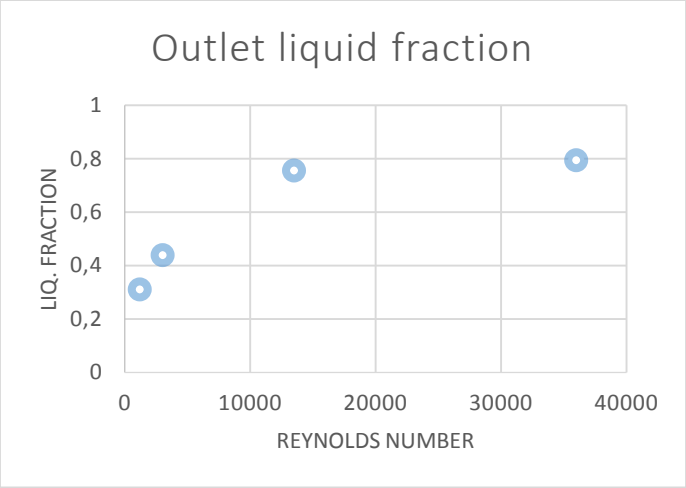

Figure 20 - Outlet liquid fraction in function of Reynolds number

It is also interesting to plot contours that reveal the buildup of ice (Figure 21).

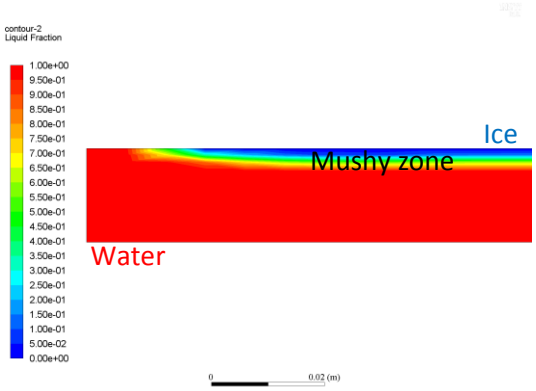

Figure 21. a) Initial formation of ice within the pipe entrance

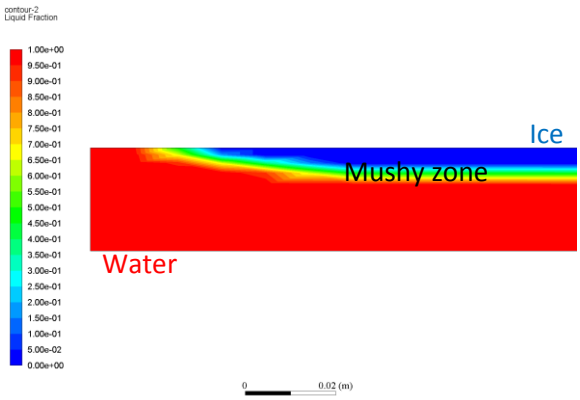

Figure 21. b) steady state at the entrance

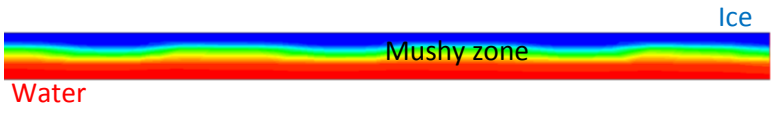

Figure 21. c) wavy behavior of ice growth analogous to Gilpin ice bands

Figure 21 - Ice growth in a pipe with initial ReD = 1200

Near the wall we can see part with liquid fraction 0, fully iced; near the axis we see the water-liquid, with solid fraction 1. Between that blue zone and the red zone, we have the mushy zone, where the water liquid is freezing.

This last Figure 21 shows the ice growth in the pipe, when Reynolds is 1,200, so a case where we have more ice. In Figure 21a I present the liquid fraction of flow in the pipe entrance after the first seconds of the simulation revealing the start of ice formation in the pipe. In the models with higher mass flows (i.e. higher Re), the start of the ice layer was farther aft from the inlet. The ice layer continues to grow until the flow develops to a steady state solution as shown in Figure 21b.

We can observe the aft end of the pipe in Figure 21c. In this image, one can see a wavy behavior in the ice growth. It was also observed at the pipe entrance. Although this behavior was not very noticeable in Figure 21a and b, it was more clear in other simulations.

A maximum thickness is reached of the ice layer near the pipe entrance, and after, it thins. This is also due to the same effect that Gilpin explained in his paper. During the growth of the ice layer, the fluid undergoes a strong acceleration in the entrance of the cooled section, this acceleration tends to laminarize the flow. Because of the flow laminarization, the laminar sublayer at the wall increases in thickness and the heat transfer from the fluid to the solid crust diminishes. The thicker laminar sublayer is stabilized by the strong negative pressure gradient in axial direction. In a distance from the entrance the ice layers get nearly parallel and the acceleration of the fluid tends to zero. Therefore, the stabilizing pressure gradient of the outer flow ceases and the fluid recedes to its originally turbulent state. The increase in heat transfer to the solid crust results in a decreasing ice layer thickness in this region. If the preceding laminarization of the fluid was moderate only, the flow passage expands gradually in the flow direction [20].

If the flow passage undergoes a rapid expansion at some point, then a flow separation will result generating a region of intense turbulence downstream. This turbulence results in a greatly enhanced heat transfer rate from the water to the ice. Further downstream, the flow will relaminarize, thus initiating a new growth layer of ice that self-perpetuates another wave.

In the following Figure 22 and Figure 23, we can confirm that this turbulence contributes to the formation of the ice-bands that we observed in our simulation. The two images are from the same part of the pipe, at the same moment. We observe that the turbulence increases when there is flow separation, and decreases as the flow relaminarizes allowing theice layer to thicken once more.

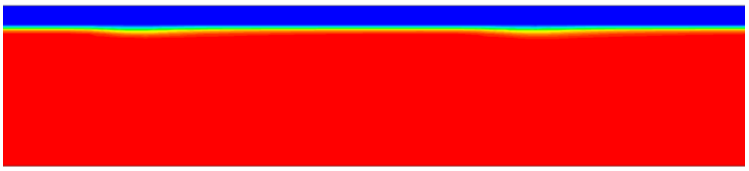

Figure 22 - Ice bands

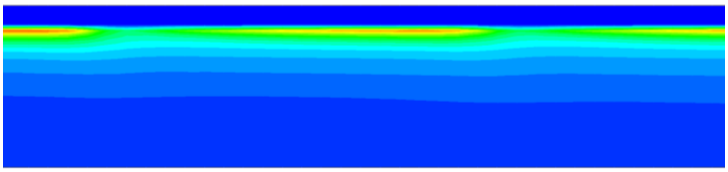

Figure 23 - Turbulence in a single pipe flow

Just to verify that our simulation make sense and looks correct, it's good to see that the pressure also increases with the thickening ice layer. This is from the 3,025 Reynolds number case (mass flow = 0.137 kg/s).

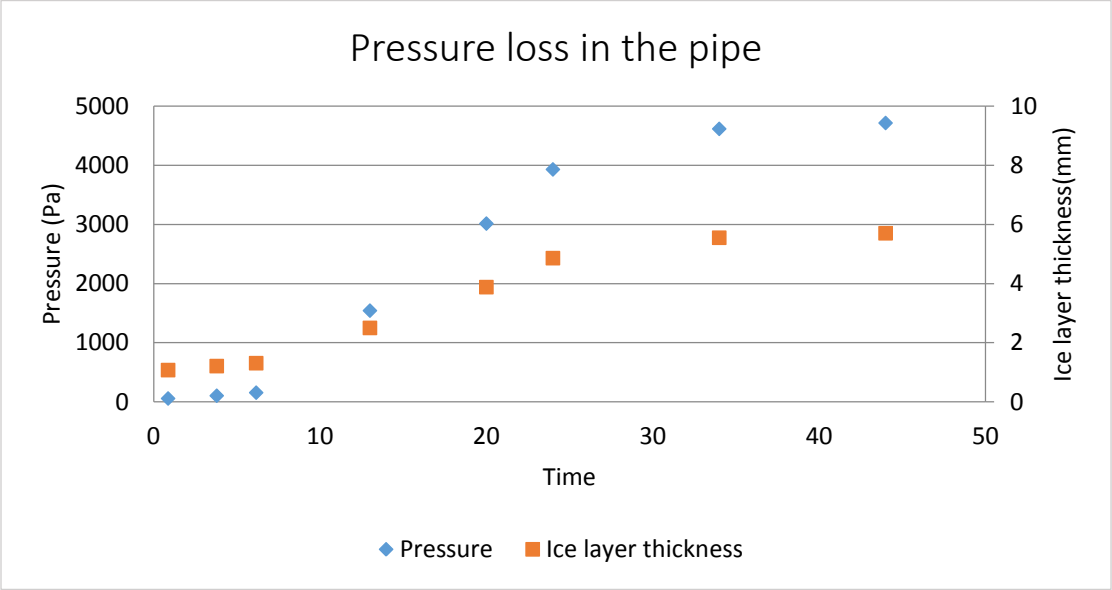

Figure 24 - Pressure loss in a single

In addition, it is nice to see that the velocity is zero in the entire ice layer, and the water only flows where the liquid fraction is not zero. In the next Figure 25, we can see the velocity vectors for the same situation of the ice growth of Figure 21 b. We can observe that there is no velocity within the ice zone.

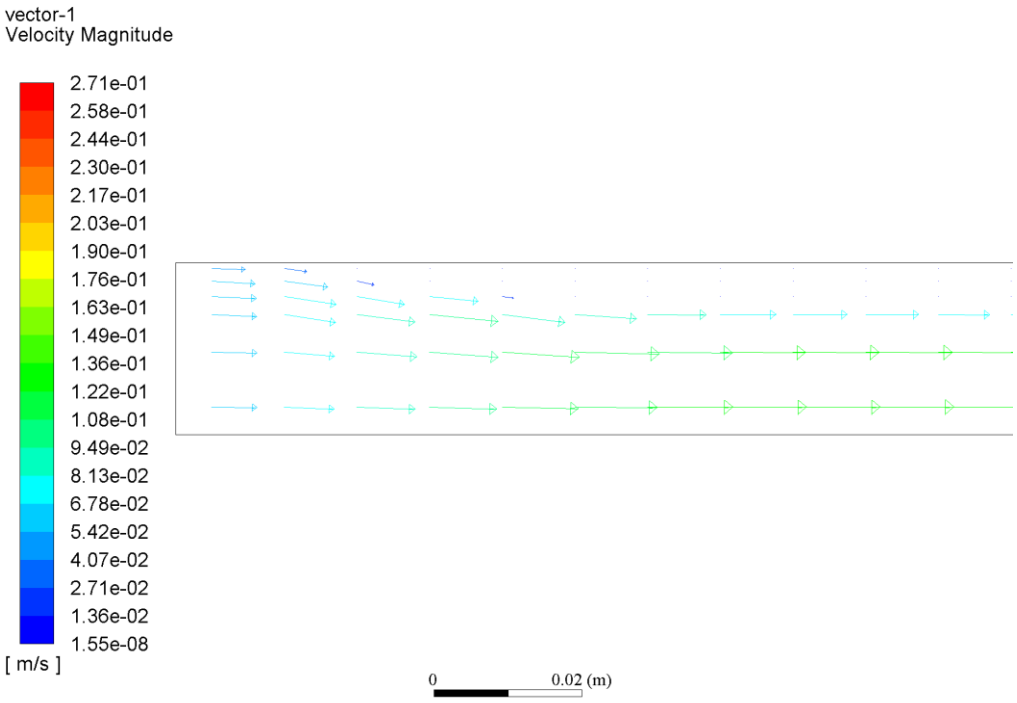

Figure 25 - Velocity of flow in a pipe with ice growth

3.2. SRHX

Our original intent was to simulate the SRHX after model validation of freezing pipe flow with Gilpin's experiments. Finally, we have focused more to analyze the solidification process of water in a cylindrical pipe and understand the effects of different parameters on the freezing of water in a pipe. And, although we achieved good results, they are not yet mesh independent results, as we were not practically able to simulate the flows with a more refined mesh and with smaller time step due to our limited computational capacity.

The same problem exists with the 3D model of the SRHX. As it is not symmetrical about an axis, I cannot do a 2D model. Still, I would like to model the heat exchanger and simulate the flow with goal to achieve a reasonable solution. Moreover, as it is a 3D model, I will need a lot more mesh elements, which will further slow the computational speed needing more time to get solutions. As it turned out, I needed more than a week of computational time to reach some results.

Geometry

The geometry of the SRHX was shown in Figure 8. The Al-6061 heat exchanger shell has an outer radius of 12.7 mm and is 305 mm long. The inner radius of the shell is 11.81 mm (the resulting wall thickness is 0.89 mm). Seven fins parse the flow path into six equally sized, freezable channels for the transport of heat and a single, thermally insulated channel that has a large enough cross-sectional area (twice the size of the freezable channels) to carry the water flow, even when all of the other channels are frozen. The six freezable flow channels were spaced 45 degrees apart. Each fin is 7.62 mm high×0.79 mm thick. The relatively thin fins with such large surface areas should ensure that the Biot number is much less than one. A 1.59–mm-thick layer of polytetrafluoroethylene (PTFE) was used to insulate the water flowing through the 90 degrees sector. Its thermal conductivity is only 0.25 W/m·°C. There is also room in the center of the heat exchanger for the expansion of ice during freeze. Despite its importance for ensuring the integrity of the heat exchanger structure during freeze, this component was neglected during development of the computational model.

The geometry was designed with Solid Works and was imported to ANSYS.

Mesh

I initialized a relatively coarse mesh (Figure 26) in order to reduce the computational time, yet be good enough for the simulation to capture important features of the flow.

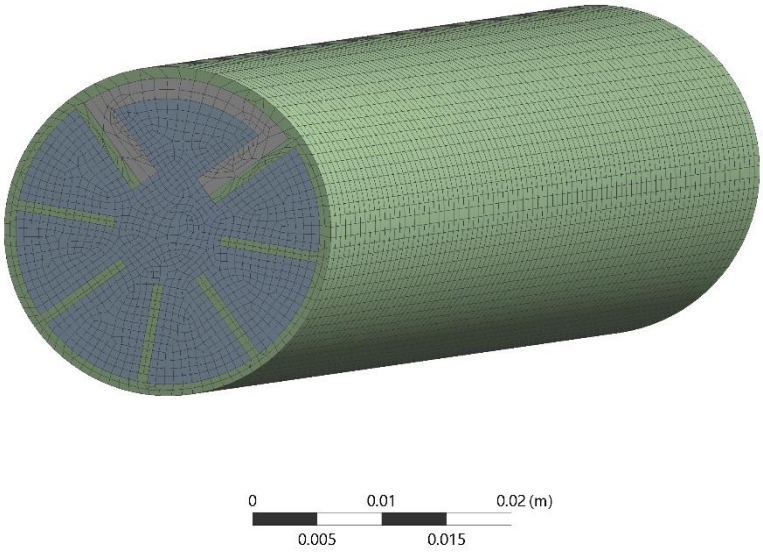

Figure 26 - Mesh for the SRHX 3D model

Set up

The model set up was quite similar to the axisymmetric 2D model.

As for the 2D model, I developed a pressure-based and transient simulation for the 3D model although now with a smaller time step for the 3D simulation. Also, I used the energy and solidification/melting models. For the viscous model, I employed the laminar and Standard k-omega turbulence models for simulations, one with a laminar flow and the other with a turbulent flow, respectively.

For the materials, a new one was introduced into the model. A polytetrafluoroethylene layer insulated the water in one flow channel from the subcooled wall. The properties introduced for this material are:

2200 kg/m3 for the density, 970 J/kg K for the specific heat, and 0.25 W/m·°C for the thermal conductivity. The properties for the aluminum and for the water are the same as used for the 2D model.

The boundary conditions were more challenging to introduce than for simple pipe flow, because the more complex finned geometry had many more surfaces. However, I was able to use the same procedure developed for the 2D model. I set constant temperatures to the heat exchanger outer wall and water inlet. Also, I defined a pressure outlet and mass flow for the water. All the boundary conditions are the same as for the axisymmetric model with exception of the mass flow through the water inlet, which was calculated for the case of interest; either a very laminar flow or a very turbulent flow as previously described. The inlet mass flow for the laminar situation is 0.00125 kg/s with a Reynolds number flow of approximately 50. For the turbulent situation, the mass flow was 0.25 kg/s.

All other model parameters were the same as for the 2D model.

Results

For the SRHX, I did not analyze the influence of the different flow parameters despite my interest. The simulation results show that the insulated channel works well, preventing the freezing of water in that channel while an ice layer formed in the other channels. We observe this phenomenon in the next pictures of the solution of the SRHX 3D model. These contour plots of liquid fraction are from the laminar flow case, the one that had more ice.

Figure 27 - Liquid fraction of the SRHX

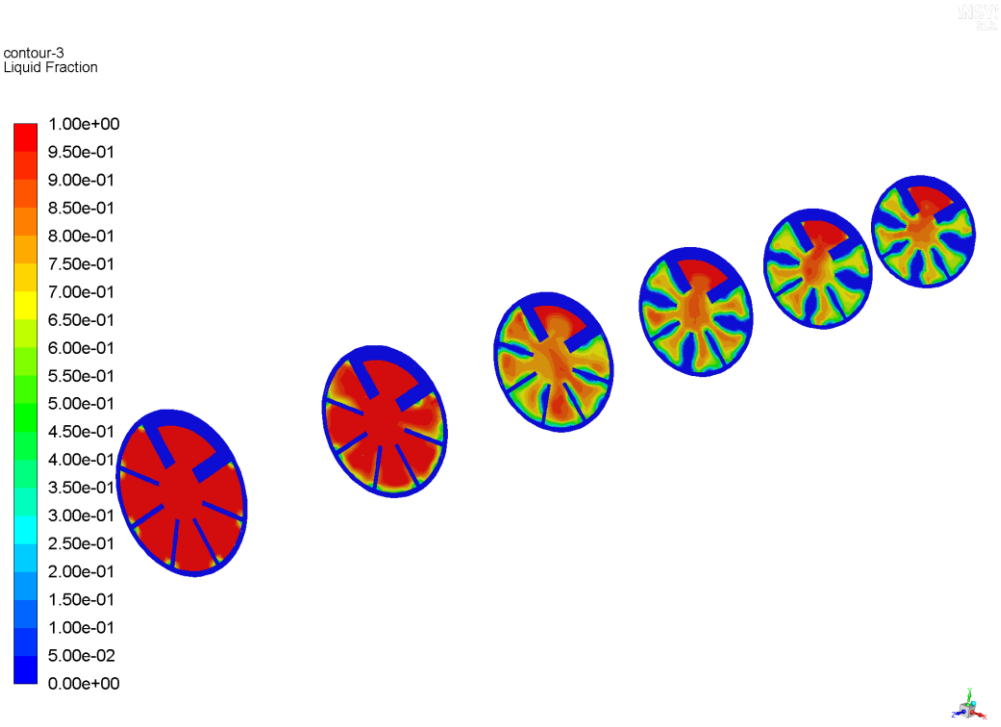

Figure 28 - Different cross-sectional cuts in the SRHX while freezing

Summary of Computational Results

Here, I make some specific conclusions about freezable heat exchanger model development and the simulation results. In my work, I found that:

- The transient simulation worked better than the steady-state simulation for stable, converged solutions of ice formation problems.
- The axisymmetric 2D simplification provided results similar to the 3D simulation, but way faster. If the problem can be modeled in 2D or, even better, with an axisymmetric simplification, it´s worth it. It saved much computational time.
- The mesh with refinement near the wall was quite good, but not good enough to reach mesh independent solutions. More computational capacity will be needed in the future to solve the problem with a more refined mesh within a reasonable time.
- The material selection and its properties worked very well except for the density of the water. ANSYS Fluent did not correctly solve the problem using temperature-dependent density data thus requiring a single value for both the density of water and ice.
- The Fluent models selected worked well. The solidification/melting model was able to solve this kind of problem. Trying to solve freezing flow with a multiphase model did not work. There are many options for turbulence models, and their evaluation was not an objective of this work. The k-omega turbulence model was used and it appeared sufficient for modeling turbulent water flow through a straight pipe.

The boundary and initial conditions were defined to match the desired flow conditions. If mesh independent solutions are reached in the future, we think that the boundary conditions reported here are reasonable for study of freezing flows of different Reynolds numbers.

Although mesh-independent solutions were not achieved, I learned how to model a CFD problem with solidification of ice and analyzed the behavior of ice growth in a single pipe, understanding the effects of the different boundary conditions and its effects on the flow behavior. In addition, the correct behavior of the SRHX and its insulated passage has been successfully verified.

Chapter 4: Experimental data. Additional experiments

4.1. Introduction

As it was explained in the background chapter, TDA Research Inc. developed a SRHX that Professor Nabity designed for use in a dual-loop thermal control architecture. The test article used a tube-in-tube design. The inner tube takes the warm water from the spacecraft, cools it by transferring its heat to the coolant in the outer tube, and then returns cool water back to the cabin. The outer tube picks up the heat load from the spacecraft and carries it to the radiator, which rejects it to space. The inner tube has fins to help efficiently transfer heat to the wall; however, the space between two of the fins is insulated (from both the wall and the fins) so that the water flowing through that channel stays above the freeze point.

In Chapter 3 I modeled the freeze of water in pipes and the SRHX. This chapter reports experimental results obtained to validate the model.

The SRHX was tested in the past to characterize its performance and understand the effects of gravity on the ice layer growth [1][2][6][20].

My main goals are the following:

In the prior experiments, dynamic disturbances or oscillations in the surface temperature were observed. Although the cause is not yet understood, it may be due to the unsteady nucleation and thaw of ice within the heat exchanger. The heat of fusion from water freezing to ice will warm the water and may melt some ice just downstream. Thus, the ice layer may thicken and thin; a cycle that repeats itself down the length of the heat exchanger.

As one of the main purposes of the computational study was to investigate the ice formation behavior, it may be interesting to repeat the experiments to see if the disturbances really come from that issue, or are due to problems with the thermistor installation (that could happen if, for example, the thermistors are not well attached to the surface). Therefore, the first goal was to repeat experiments in order to confirm if the disturbances are due to ice formation behavior or a problem with the thermistors.

Another goal is to conduct freeze/thaw experiments with turbulent flows.

Last, the SRHX experiments have been with steady state flows and heat loads, whereas transient tests are desired. It would be interesting to dynamically change conditions in order to characterize performance with different heat loads that simulate an orbiting spacecraft. As will be seen, due to problems with some components of the experimental apparatus, not all goals were successfully reached.

4.2. Elements & Assembly

In this part, the characteristics of the SRHX and of all its elements will be explained. Although many of these components were constructed or purchased in the past, we needed some new elements, and the assembly was done again, starting from scratch.

The PID of the experimental test is shown below, in Figure 29.

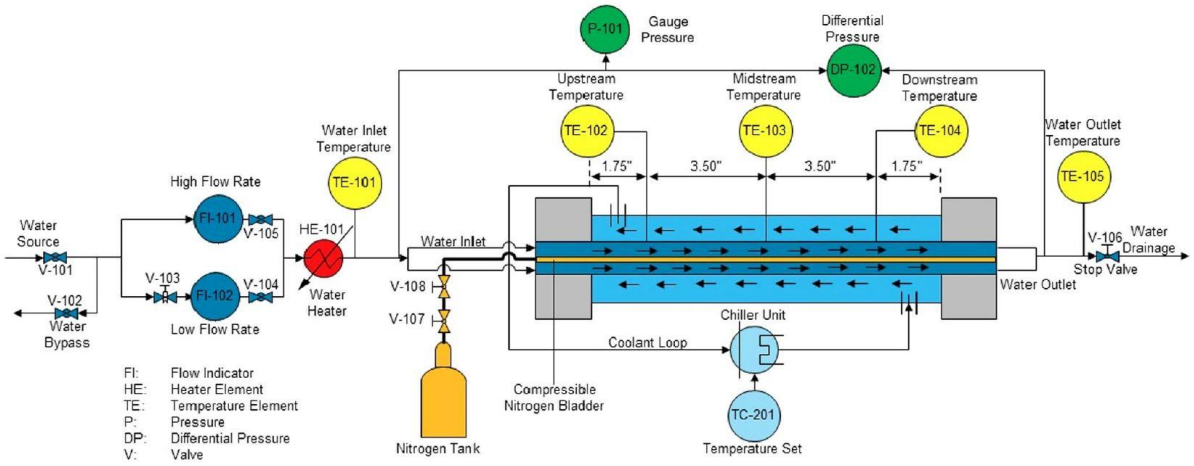

Figure 29 – PID of the freezable heat exchanger [1]

Inner tube

The inner tube of the heat exchanger is the most important part of the SRHX. As it was said, it's made of Al-6061, it has an outer radius of 12.7 mm and is 305 mm long. The inner radius of the shell is 11.81mm (the resulting wall thickness is 0.89 mm). Seven fins parse the flowpath into six equally sized, freezable channels for the transport of heat and a single, thermally insulated channel that has a large enough cross-sectional area (twice the size of the freezable channels) to carry the water flow, even when all of the other channels are frozen. The six freezable flow channels were spaced 45 deg apart. Each fin is 7.62 mm high × 0.79 mm thick. A 1.59–mm-thick layer of polytetrafluoroethylene (PTFE) was used to insulate the water flowing through the 90 degrees sector. The wires wrapped around the tube trips the laminar flow to turbulent to significantly increase the heat transfer. We can see this inner tube in the following Figure 30. (The white wires of the image are the thermistors, attached to the surface, which will be explained later).

All the dimensions were measured with an accuracy of ± 0.0013 mm except the length of the heat exchanger that measures 304.8 ± 0.3 mm.

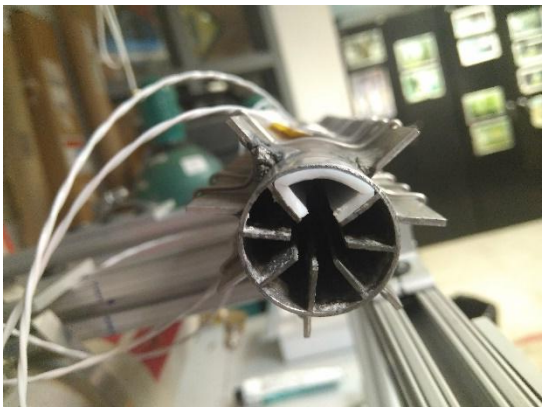

Figure 30 - Inner tube of the heat exchanger

Shell

The inner tube was situated inside the shell (Figure 31), where the coolant flows. This shell is made of PVC.

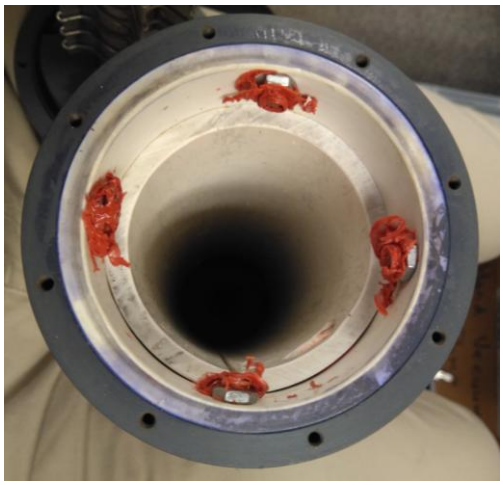

Figure 31 - Shell of the SRHX

Thermistors

A thermistor is a type of resistor whose resistance is dependent on temperature, so we can use them as a temperature sensor. Typically, for this purpose, NTC (negative temperature coefficient) thermistors are used. In NTC thermistors, resistance decreases as temperature rises.

Three Omega SA1-TH-44004-40-T thermistors were secured to the outer wall of the finned heat exchanger tube for measurement of surface temperatures along the heat exchanger's wall. Two thermistor probes were used to measure the inlet and outlet water temperatures.

For both types of thermistors, we need a conversion table or equation to convert from resistance to temperature; this table/equation was given by the manufacturer.

A LabVIEW program collected the data from these thermistors, and converted voltages to temperatures. Data acquisition devices (DAQs)measured voltages, but not thermistor resistances. I thus designed a circuit to collect voltages s and from these values get the resistances, and after, the temperatures.

The most common circuit to do this is the well-known Wheatstone bridge, a simple circuit for measuring an unknown resistance by connecting it to form a quadrilateral with three known resistances and applying a voltage between a pair of opposite corners. We can see a diagram of this circuit in the following Figure 32.

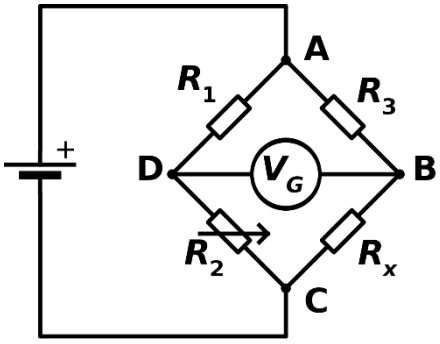

Figure 32- Wheatstone bridge diagram

In Figure 32, R_1, R_2 and R_3 are resistors of known resistance, and R_x is the thermistor, so the resistor which we do not know its value. We used the same values for R_1, R_2 and R_3 in order to simplify the equation used to obtain the value of Rx. We can see this equation below.

$$V_G = \left(\frac{R_2}{R_1 + R_2} - \frac{R_x}{R_x + R_3}\right) V_s$$

Measuring the values of V_G will allow us to obtain the value of R_x with the help of our LabVIEW program. We will talk about this program later.

Five Wheatstone bridges were needed in order to measure the five temperatures. We used two breadboards and two DAQs to measure the voltages and collect the data in our computer. We can see a picture of the Wheatstone bridges and the DAQs below.

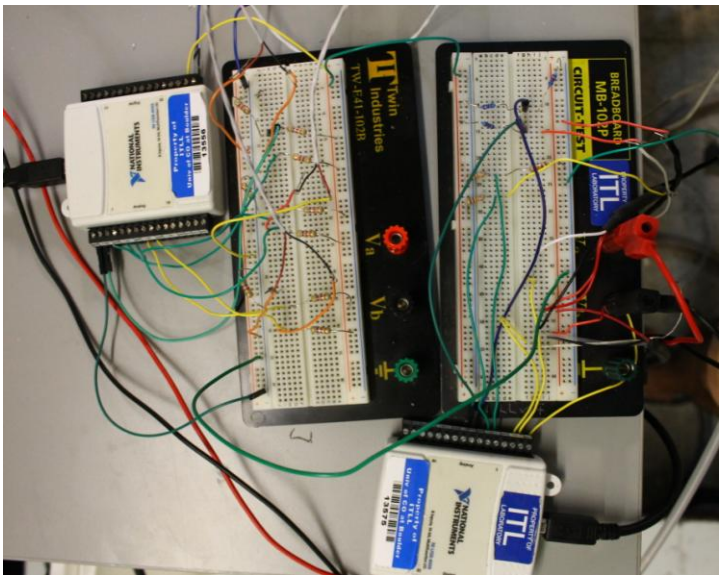

Figure 33 - The two breadboards and the two DAQs used for the data collection

In the left breadboard of Figure 33 we can see three Wheatstone bridges for the three surface temperatures, in the right breadboard we can see two more, one each for the inlet and outlet temperatures.

In this last Figure 33, we can see part of the surface thermistors (the white wires that divide into a black and red wire); the other end of the wire is the part sensible to temperature, which is attached to the surface. The challenge is attaching it securely without leaving any free space between the thermistor and the surface; with this purpose, we decided to use a very thermally conductive compound at the contact surface, and afterwards we used J-B Weld epoxy to attach all the thermistors to the surface. In the following Figure 34, we can see part of the inner tube with the thermistors attached, waiting for the epoxy to dry before introducing the tube into the shell. One of the thermistors is in the center of the tube, the two others 102 mm from the center.

Figure 34 - Inner tube with the thermistors attached to the surface

The two thermistors for the inlet and the outlet of the water measure their respective temperatures with ± 0.15°C accuracy. The three surface thermistors measure their temperatures with ± 0.2°C accuracy.

Pressure transducers

A pressure sensor is a device for pressure measurement of gases or liquids. Pressure sensors are commonly called pressure transducers. Pressure sensors can vary significantly in technology, design, performance, application suitability and cost; thus choosing the right transducer is important. Two Omega transducers were used, one for the inlet pressure and another one for the pressure difference between the inlet and the outlet.

PX309-030G5V (0-30 psi gauge transducer)

PX409-015DWU5V (0-15 psid differential transducer)

These measure the pressure changes during freeze, as the ice blockage will lead to an increase of the pressure difference between the inlet and the outlet.

The manufacturer provided calibration data to transform measured voltages to pressure values; also, we will use the DAQs and the LabVIEW program for the data acquisition. We can see the wires of the pressure transducers connected to the breadboard (Figure 33, bottom of the right breadboard). a 30 VDC power supply provided the 10V excitation voltage needed by the transducers.

We can see in the following Figure 35 the two transducers connected to the circuit, measuring the inlet pressure (P101) and the differential pressure (DP102) between inlet and outlet.

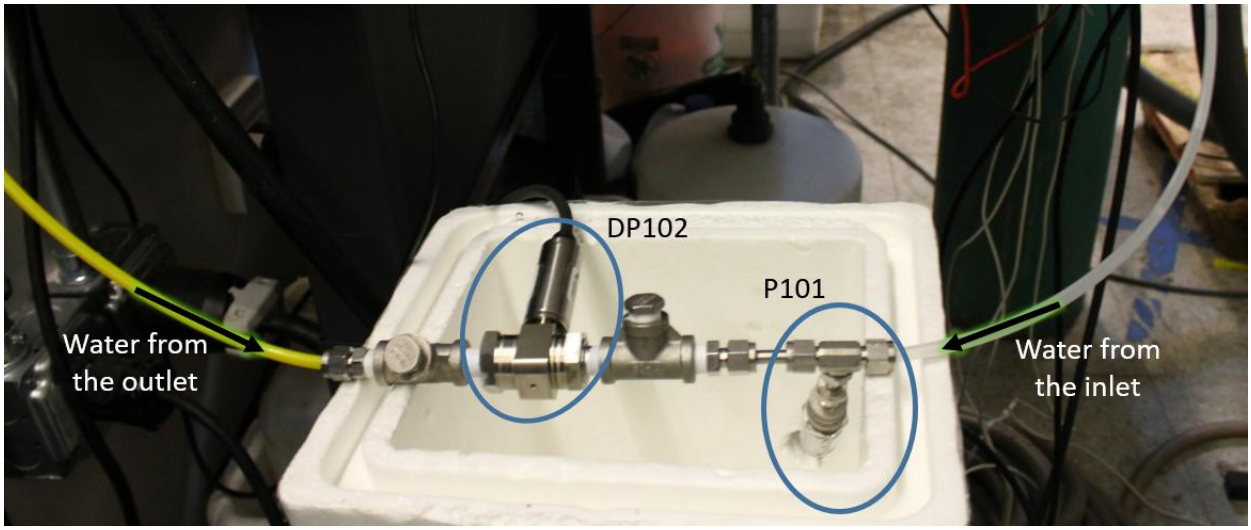

Figure 35 - Pressure transducers

The accuracy of the differential pressure transducer is 0.08% and the accuracy of the gauge pressure transducer for the water inlet is 0.25% of full scale.

Rotameter

A rotameter is a device that measures the volumetric flow rate of fluid in a closed tube. It belongs to a class of meters called variable area meters, which measure flow rate by allowing the cross-sectional area the fluid travels through to vary, causing a measurable effect.

Accurate flowmeters were desired for digital acquisition of the mass flow data while the experiments were running. Nevertheless, all lab flow meters were broken, and so a less accurate, analog flow rotameter was used to periodically check the mass flow value. An inhouse calibration was performed by comparing the time needed to fill one liter of water with the value given by the rotameter. Although the differences were about 5%, never more than 10%, the repeatability was good enough to use the device. In every experiment, the water was also measured by looking at how much water we can fill with a specific mass flow, to verify the value given by the rotameter. With this action, the accuracy depended on the range. It varied from 2% to 5%.

Uncertainty quantification

For the different parameters measured with our thermistors, transducers and rotameters, we have talked about their uncertainties. In some cases, this uncertainty was given by the manufacturer (i.e. thermistors and transducers) and in other cases the uncertainty was measured (rotameter).

The uncertainty of these variables will affect the uncertainty of other parameters calculated from these variables.

In the following table, we can see all the variables used and their associated errors. The uncertainty of the variable is displayed in the final column. This uncertainty can be given, measured, or calculated. If calculated, the variables have uncertainty percentages, based upon an uncertainty model.

$$uncertainty = 2sqrt\left(\frac{meas_1}{uncertainty_1}^2 + \cdots + \frac{meas_n}{uncertainty_n}^2\right)$$

The uncertainty equation calculates the sum of squares for each value, based on the magnitude of the value, and the uncertainty of the value. The summation of each squared value is determined, at which point the square root is taken of the result. The final result is then multiplied by 2, since the uncertainty is an absolute value, and can become either positive or negative when implemented in further equations.

Variable	Description	Units	Measured, given, calculated	Value	Uncertainty
m_{wf}	Mass flow rate of water through the heat exchanger	l/min	Measured	0.2 / 0.4	2%-5%
T_{in} , T_{out}	Inlet and outlet temperatures	C	Given		0.15
T_{102} , T_{103} , T_{104}	Surface temperatures	C	Given		0.2
ΔP	Pressure loss across the heat exchanger	psi	Given		0.08%
P	Pressure inlet	psi	Given		0.25%
C_p	Specific heat of water	J/kg	Given		20
k	Thermal conductivity of the heat exchanger	W/m-K	Given	167	1
H	Heat of fusion of water	J/kg	Given	334000	1000
Q	Heat transferred from the working fluid	W	Calculated		2.6-12.3%

Table 2 – Variable definitions and uncertainties

Nitrogen tank

We used a pressurized bladder to provide room for the volumetric expansion of water to ice. A regulated cylinder of gaseous nitrogen (Figure 36) inflated the bladder to 17.2 kPa (2.5 psi) above the water pressure within the heat exchanger.

Figure 36 - Nitrogen Tank used for our tests

Chiller unit

A chiller unit was used to lower the coolant temperature to -20°C. The coolant was a 60/40 mixture of propylene glycol and water. The chiller was a Thermo Haake C50P, that we can see below in Figure 37. The chiller rejected the heat from the heat exchanger to the surroundings. The coolant recirculation pump was set to its maximum flow capacity, at approximately 24 l/min.

Figure 37 - Chiller used for the experiments

The main problem I had in this experimental part was that the chiller did not have enough capacity to lower the coolant temperature to the desired set point. For our specific water mass flow, the chiller was unable to subcool the inner tube below the freeze point of water.

LabVIEW

A LabVIEW program was designed to collect the data, and to convert the different voltages to the desired units. We used two DAQs, the first one was used for the three surface thermistors, the second one for the other two thermistors and for the pressure transducers.

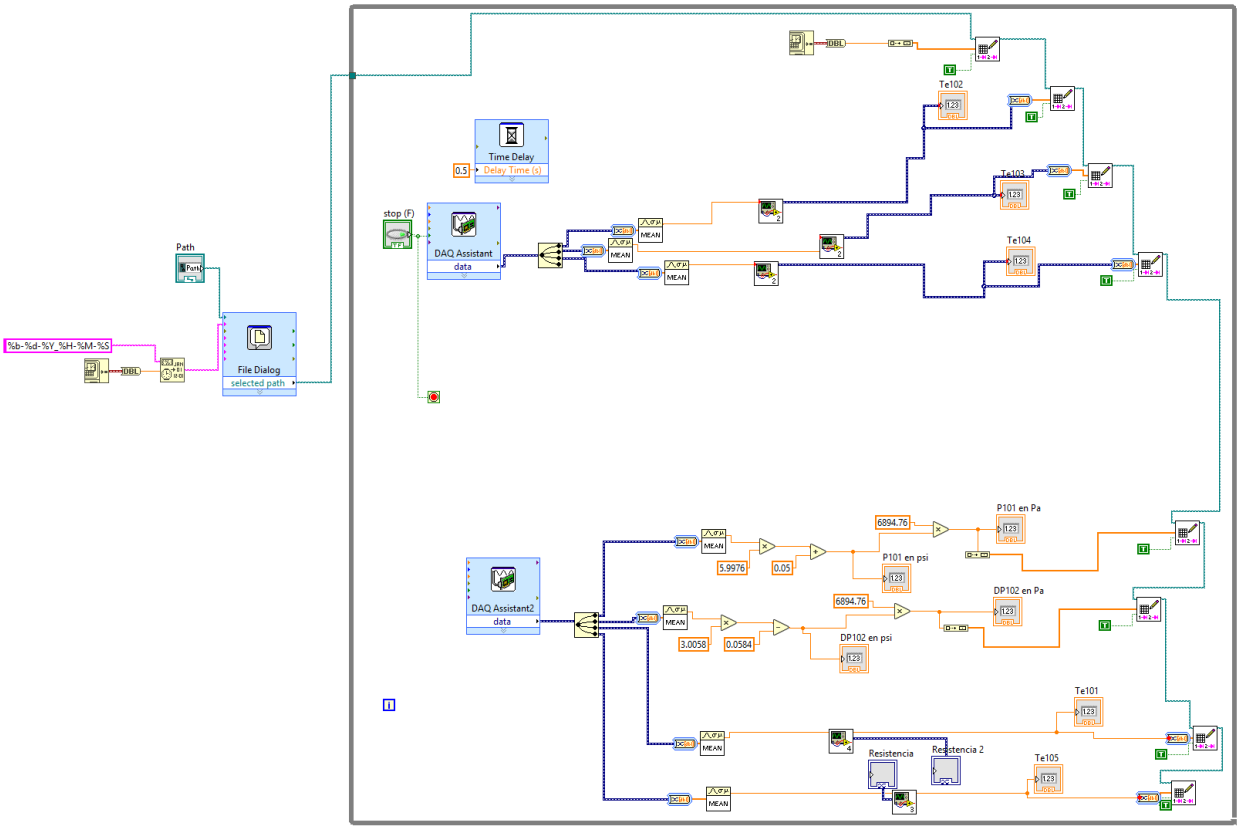

Figure 38 - LabVIEW program for the experimental tests

The designed LabVIEW program (Figure 38) automatically created a spreadsheet, where all the parameters were saved in their desired units, every 0.5 seconds. The part inside the grey square is the

loop that collects the data; the outside part is not a loop, but rather initiates the program and creates the spreadsheet. We can see two different parts inside the square, the part in the top is our first DAQ, which collects and converts the data of our three surface thermistors. The part in the bottom collects the data of the two transducers and the two other thermistors. There are some sub programs in this program, for every thermistor, to convert from voltage to temperature; these subprograms are represented with an icon in last Figure 38. We can see the subprogram in the following Figure 39. The numbers used in these subprograms vary according to the resistances used for every Wheatstone bridge.

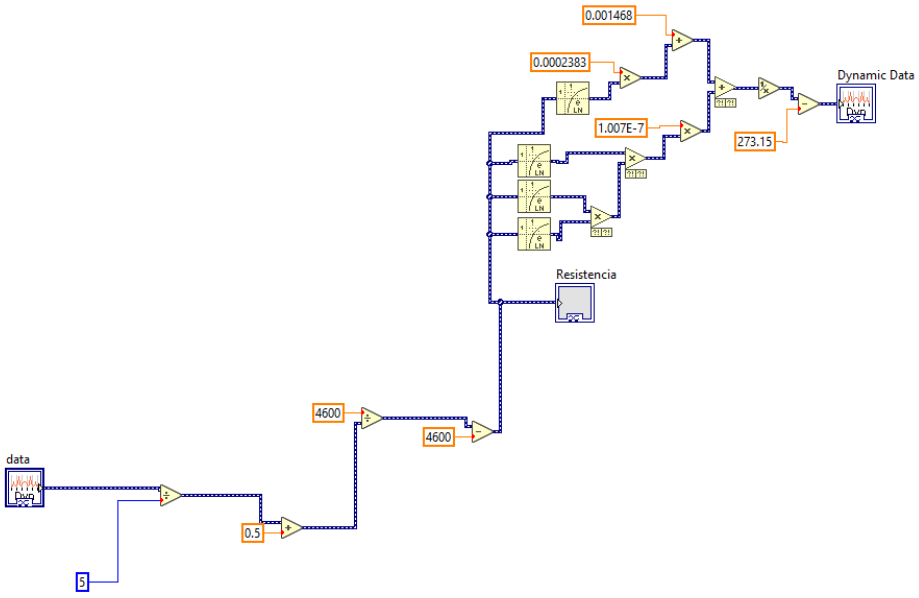

Figure 39 - Subprogram for the thermistors

In this sub program the voltage data is being converted first to resistances (left and bottom part of this Figure 39), and afterwards from resistances to temperatures (right and top part of this Figure 39) using the equation given by the manufacturer.

Final Assembly

The physical layout of the SRHX test rig and the author are shown below in Figure 40. In addition, we can see in Figure 41 and Figure 42 parts of the setup, with some explanation, in order to understand more the test apparatus.

. 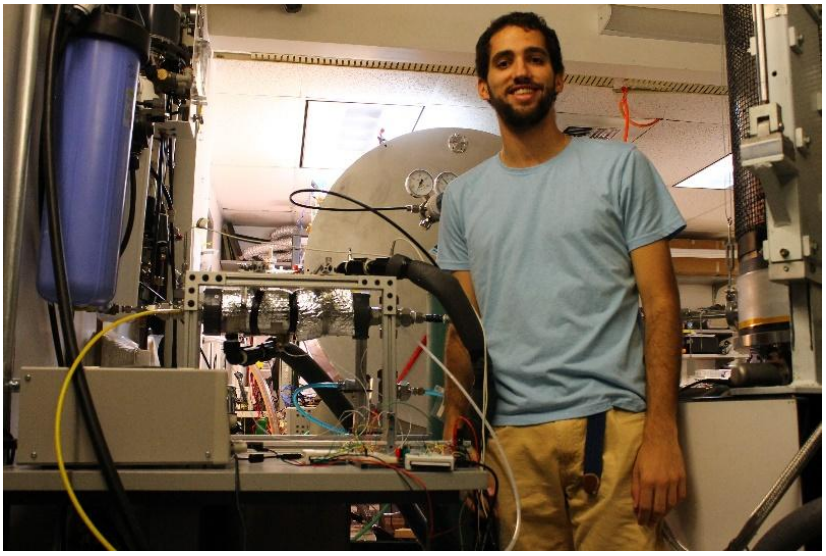

Figure 40 - SRHX test rig and the thesis author

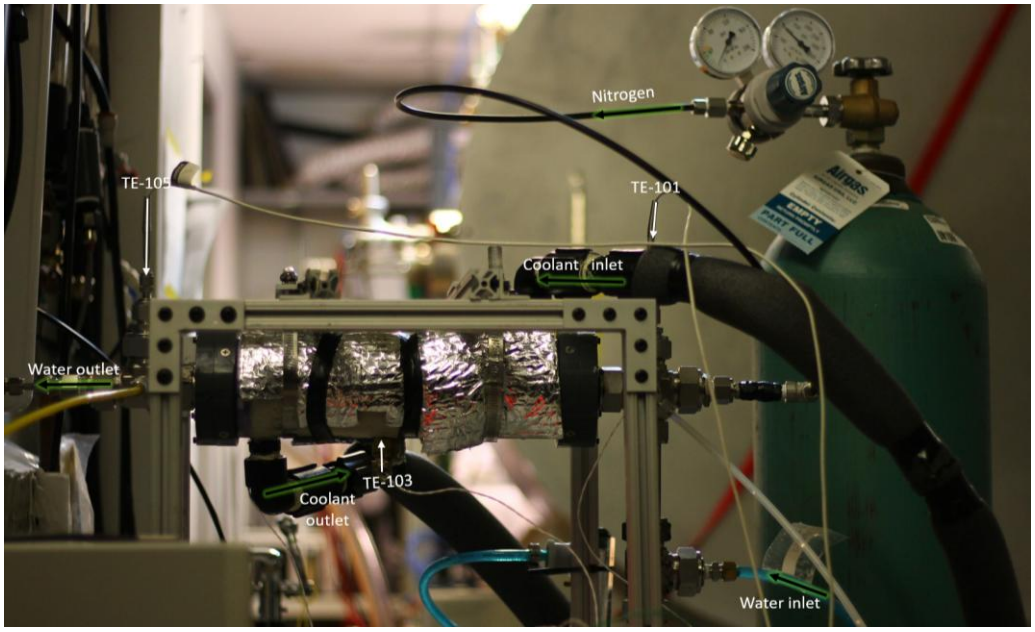

Figure 41 - SRHX

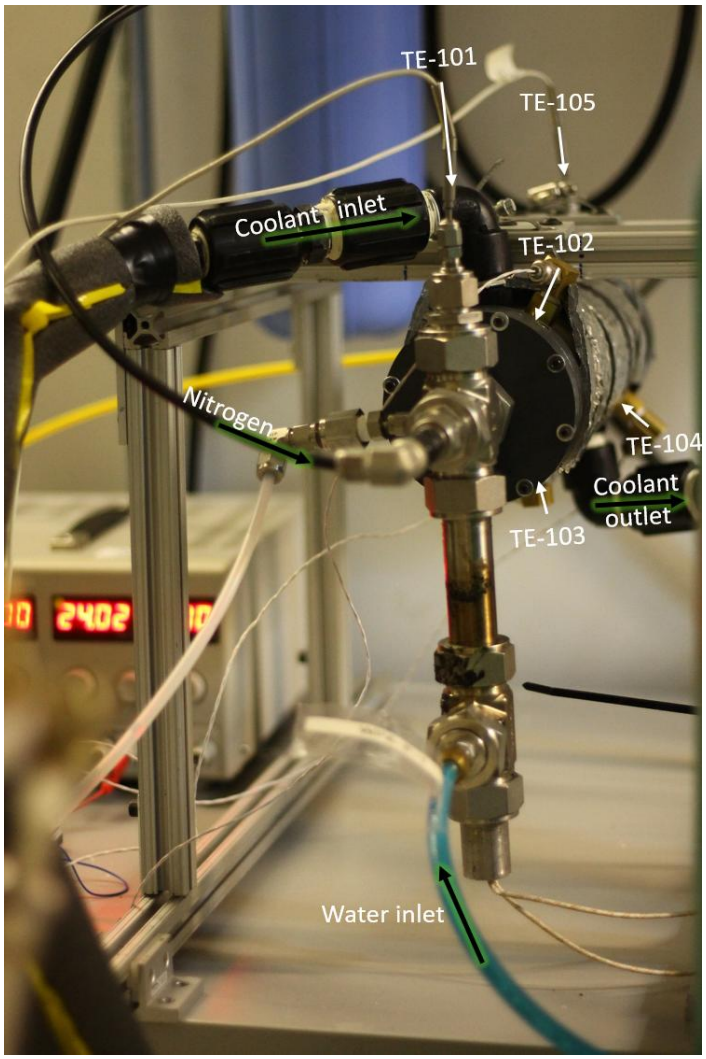

Figure 42 - SRHX

At this point, with the SRHX completely assembled, I was ready to begin the experiments.

4.3. Tests & Results

Experimental procedure

Once the SRHX was assembled, I proceeded to the experiments using the procedure reported by Professor Nabity [1]:

1) Activate the data acquisition/input–output and begin recording data.

2) Turn on the chiller and adjust the set point to 5°C.

3) Turn on the water flow to the heat exchanger and adjust to the desired test value.

4) Once the chiller reaches 5°C, keep the conditions until all temperatures had reached steady state, once they reach it, wait 5 minutes.

5) Adjust a new set point for the chiller, -20°C, to initiate freeze.

6) Wait until ice formation. This phase change was indicated by increases in the downstream water temperature, the upstream water pressure, and the differential pressure across the heat exchanger (HX). This was then followed by a small (approximately 1–2°C) rise in the heat exchanger surface temperatures due to the energy release from the heat of fusion of ice. Further, the outlet water temperature also increased and gradually reached equilibrium at a temperature only a few degrees below the inlet as ice built up within the flow channels. We allowed the experiment to continue until all temperatures and the gauge and differential pressures had reached new steady-state values for the frozen state.

7) Increase the flow rate in order to thaw all the ice. Once thawed, set the chiller again to 5°C, and start again.

Although the first time that these experiments were made all the process took 2 hours, we needed twice the time just to reach the beginning of the ice formation, due to the low capacity of the chiller used. I was not able to complete a full cycle with these conditions. A test was run, but without reaching frozen steady state conditions.

Results

As it was explained, I had problems due to the low refrigeration capacity of the chiller. It could not decrease the coolant temperature to -20°C, especially when for test conditions with high water mass flow. With turbulent flows I could just obtain a coolant temperature of -10°C. With lower mass flows, in laminar conditions, the coolant temperature of -16°C was obtained, which resulted in a wall temperature of approximately -10°C. With these conditions I was able to reach the beginning of the freezing, but not a steady state with a big part of the HX frozen.

Given the limitation on heat transfer imposed by the chiller, I needed to descope my research plans and focus on one goal: repeat the experiments to observe oscillations and determine their cause whether related to ice behavior or some other cause. Fortunately, a steady state response was not needed.

I ran several experiments. The more useful ones were the ones with more laminar flow, because it was possible to drop the heat exchanger temperatures below the freeze point. The more interesting results of these experiments are shown below. In Figure 43 we can see the results with 0.4 l/min and in Figure 44 the results with 0.2 l/min.

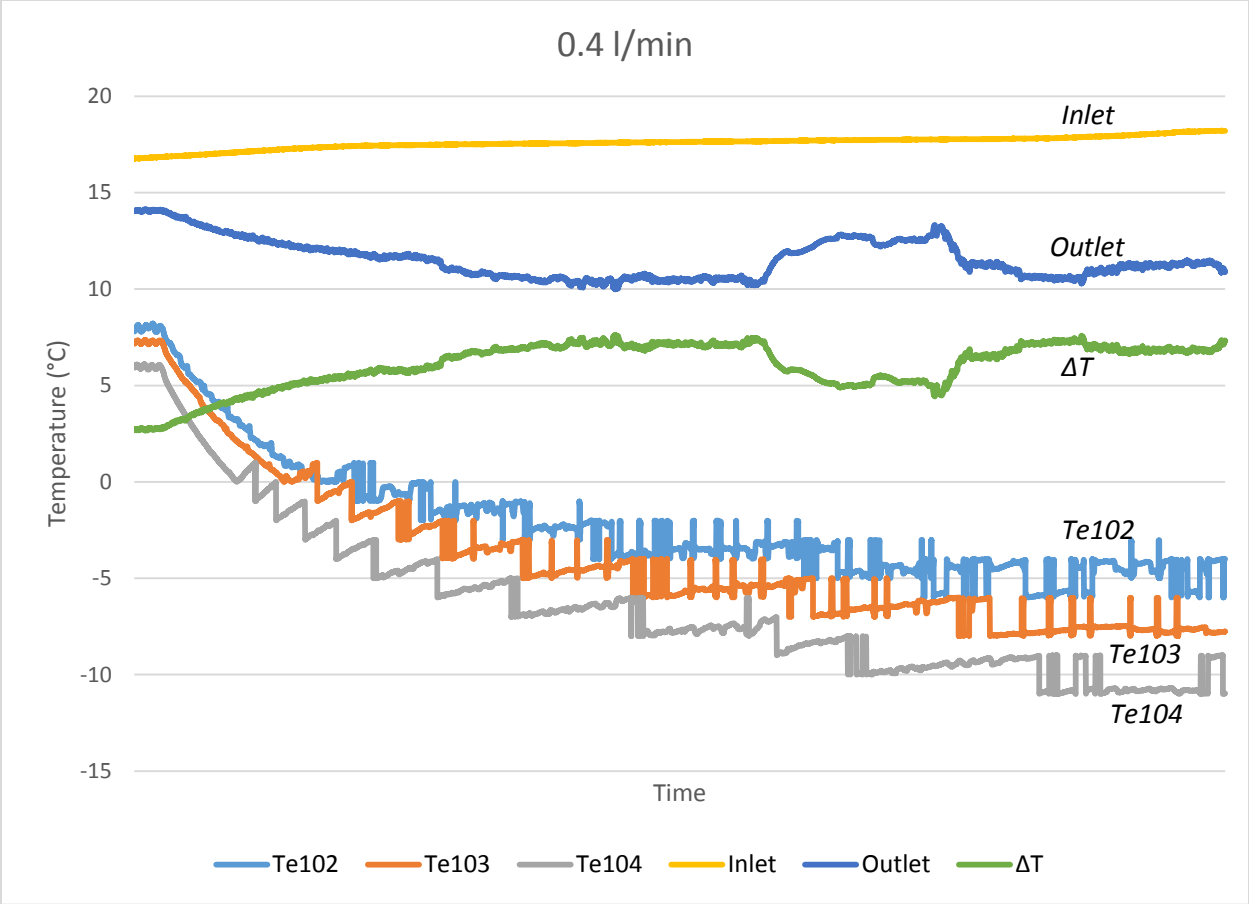

Figure 43 - Results with 0.4 l/min (ReD ≈ 100)

In this last Figure 43 we can see a graphic where the vertical axis is the temperature and the horizontal axis is time. The yellow line represents the water inlet temperature, that as you can see is approximately constant with a value of 17.5°C. The blue line is the water outlet, that starts with a value of almost 15 degrees, and decreases until the icing starts. When the ice layer starts to grow the water outlet increases due to the heat released in the phase change, because the heat of fusion from water freezing warms the water. Afterwards, as the chiller was not able to keep cooling the system, the freezing does not reach a steady state. The green line is the temperature difference between the inlet and the outlet.

As one can see, all the surface thermistors (TE102, TE103 and TE104) have a weird behavior. At first glance, it could look that there is some problem that is making the solution oscillate, maybe some electronic issue of the circuit that measures the thermistors temperature, or some problem with the

attachment of the thermistors to the heat exchanger wall. However, we can see that the oscillations occur in every thermistor just when they reach the freezing point of water. That makes us confirm that their oscillatory response may depend upon the growing ice layer. Presumably, these disturbances may arise from the unsteady nucleation and thaw of ice within the heat exchanger. The heat of fusion from water freezing to ice will warm the water and may melt some ice just downstream. Thus, the ice layer may thicken and thin; a cycle that repeats itself down the length of the heat exchanger. We can see the same effect in the 0.2 l/min experiment.

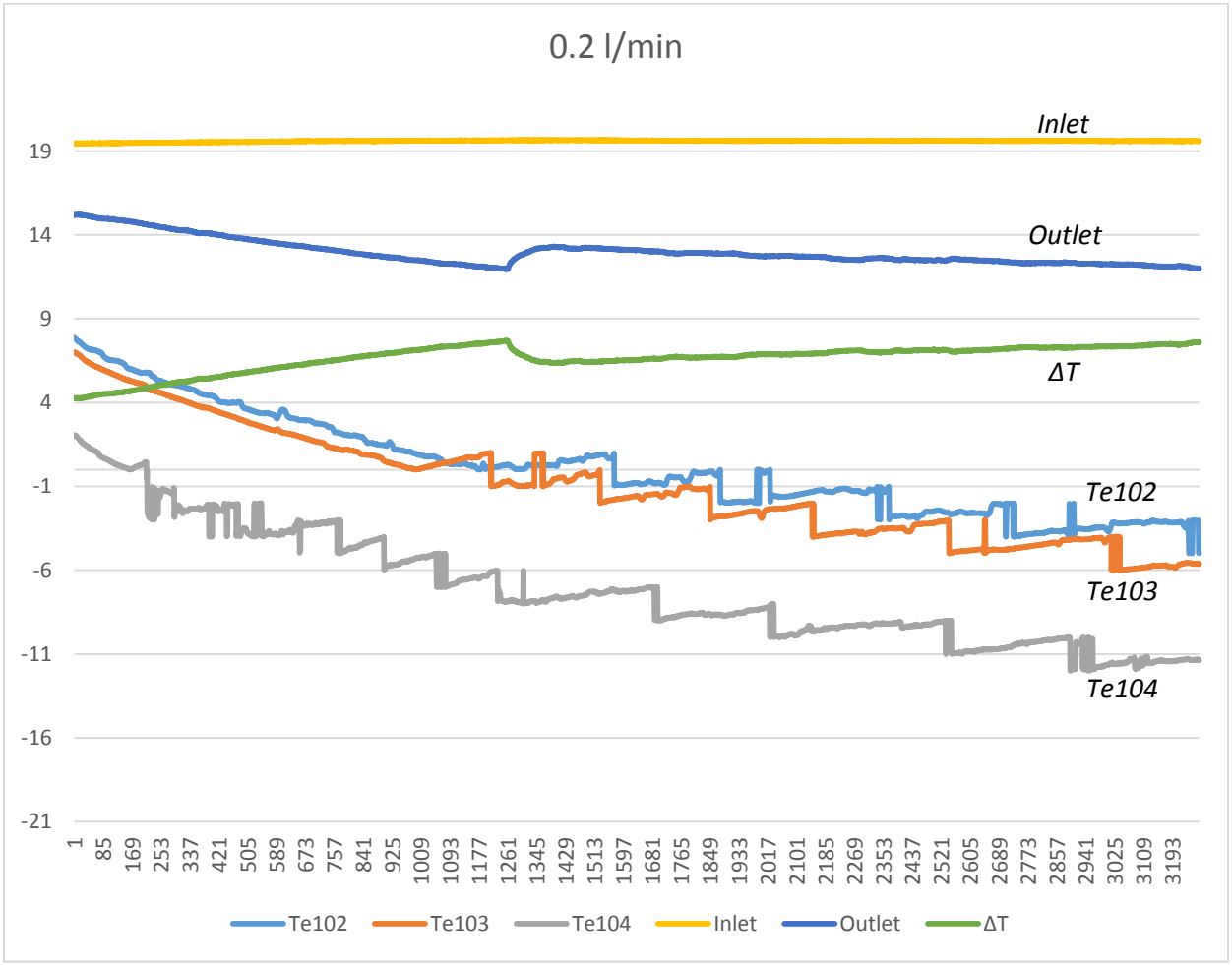

Figure 44 - Results with 0.2 l/min (ReD ≈ 50)

As we can see in Figure 44, the thermistors started oscillating also when they reached the freezing point of water, which confirms our hypothesis.

Lastly, in Figure 45 we can observe the temperature of only one of the thermistors, for another experiment, from the beginning of the test, when neither water nor coolant was flowing, at +21°C. As we said in our test procedure, we started lowering the coolant temperature to +5°C and waited until the thermistors reached steady state. For this reason we can see that as the temperature of the wall reached approximately +6.5°C it stopped decreasing for a few minutes. Afterwards, the chiller was set at -20°C, and the thermistor outputs decrease until the chiller cannot keep decreasing more. In this Figure 45 it is even clearer that oscillations begin only once the wall temperature reaches 0°C.

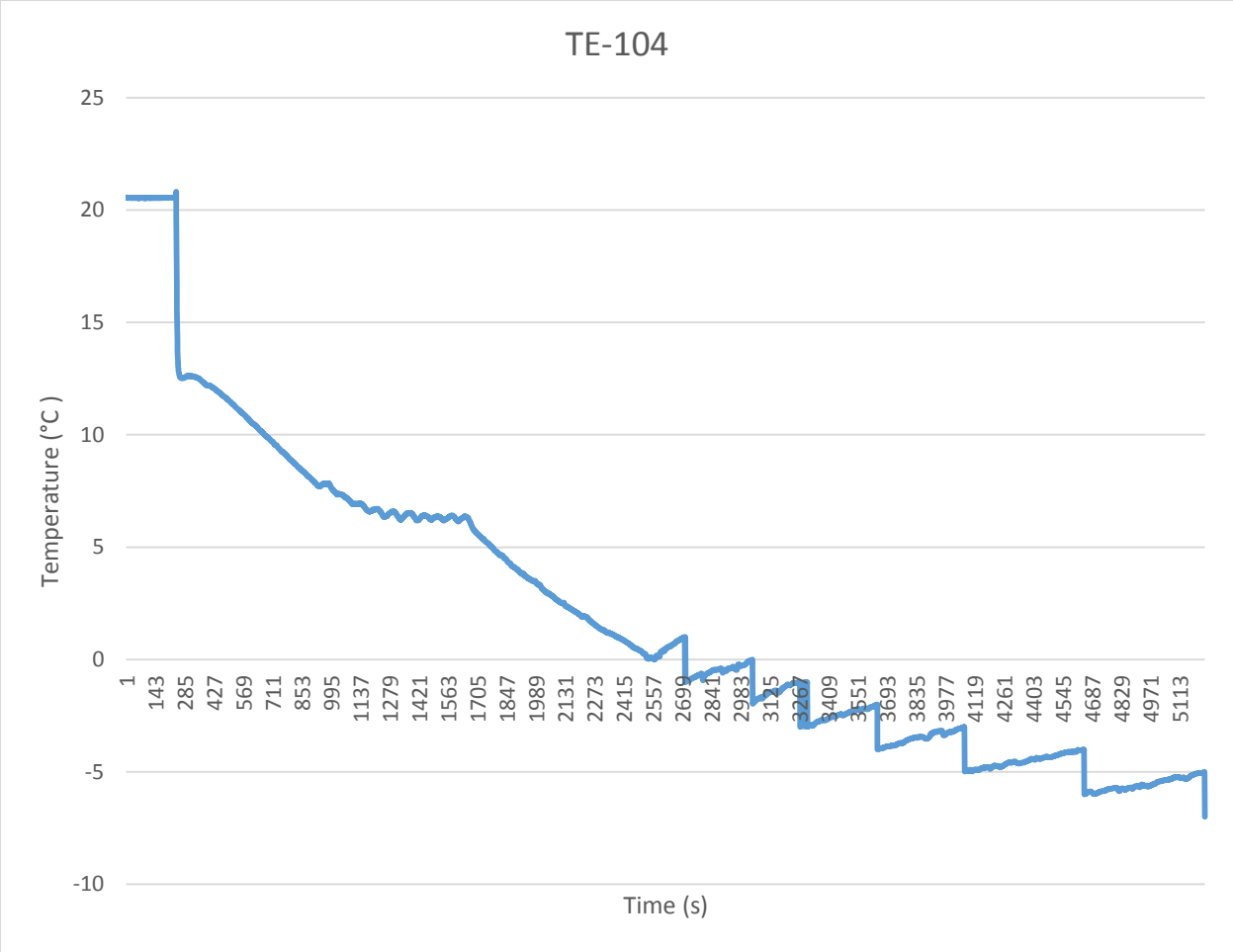

Figure 45 - Thermistor Te104 in one of the experiments (0.4l/min; ReD ≈ 100)

This unsteady ice-layer growth, observed in our computational analysis and in our experiments, needs further investigations. Maybe the same experiment should be done in the future with glass to enable direct visual observations of the phenomena occurring within the interior of the heat exchanger as ice begins to form on the walls.

Apart from this interesting issue, other aspects were observed: the heat rejection (Q) decreases when the ice starts growing; also, as it grows, the differential pressure and the inlet pressure both increase, as expected.

For the situations experimented with more turbulent flows (up to 1 l/min), the results were similar, but I was not able to reach low enough temperature to initiate freeze. Therefore, it was not possible to compare time to freeze or temperatures reached as a function of turbulence, as I would have liked. In the future, it would be interesting to test at turbulent flow conditions.

Anyway, despite the low capacity of the chiller, I conducted experiments employing several measures to lower the wall temperature and reach conditions able to freeze water: lower the water inlet temperature with an ice bath at the inlet, insulate the heat exchanger to reduce heat gain from the surroundings, and lower the coolant temperature before starting the experiment. Unfortunately, my test window ended before successfully implementing these strategies. More efforts will be necessary in the future to reach the other goals of this experimental effort.

Chapter 5: Conclusions

A freezable heat exchanger was computationally modeled and experimentally tested in order to prove its feasibility for spacecraft thermal control. As stated in the introduction of this thesis, my main goal was to characterize its performance when part of a single loop architecture for the thermal control system of a spacecraft. Therefore, this thesis contributes to the growing body of work to develop and characterize freezable heat exchangers for spacecraft thermal control. In my computational chapter, I describe an approach to model a CFD problem with solidification, in this case with ice formation, and then used the model to analyze the behavior of ice growth in a single pipe, understanding the effects of the different boundary conditions. I focused especially on studying the influence of flow turbulence on the ice growth and its behavior. The model was used to predict the ice blockage or the liquid fraction as a function of the Reynolds number. I also studied the ice-bands observed by Gilpin in his experiments, and the relation of the ice bands with the turbulence of the flow.

The SRHX was also computationally modeled, and although I did not reach mesh independent solutions, the correct behavior of the insulated passage was successfully verified for several mass flows. In the future, the freezable pipe and heat exchanger models should be simulated with more powerful computers, in order to increase the mesh refinement and reduce the time step to get more accurate solutions, and thereby confirm that the model is simulated correctly. Once designed and compared with experimental results, the model should be able to predict many different situations to simulate its behavior in space conditions.

In the experimental part, I started with three goals. The first goal was to repeat prior experiments in order to confirm if oscillations observed in the surface temperatures were due to unsteady behavior during ice formation or a problem with the thermistors. My experiments showed the onset of

oscillations in the wall temperature measurements only as the wall temperature fell below 0°C, the point at which water could just begin to freeze. It looks like the disturbances may arise from the unsteady nucleation and thaw of ice within the heat exchanger. The heat of fusion from water freezing to ice warms the water and may melt some ice just downstream. The thickening ice layer reduces the cross-sectional flow area, which then increases velocity and turbulence of the flow. If sufficient heat transfer, then this too can cause a downstream band of ice to melt raising the wall temperature within that region. Thus, the ice layer may thicken and thin; a cycle that repeats itself down the length of the heat exchanger. My experiments confirm the observation by Gilpin of traveling ice bands (or waves) in freezing pipe flow through the self-regulating heat exchanger; an interesting phenomenon that should be studied further.

Unfortunately, the low capacity of the chiller used in my freeze experiments prevented me from achieving the two other goals for the experimental part: 1) to conduct experiments with more turbulent flows and 2) the further study of transient effects during freeze and thaw.

Including my experiments, the self-regulating freezable heat exchanger has now endured well over 200 freeze/thaw cycles without damage; further proving the feasibility of this technology for use in single-loop spacecraft thermal control architectures.

Bibliography

[1] Hecht, J. B. (2012), "First Order Feasibility Evaluation of a Water-Based Freezable Heat Exchanger for Use in Human Spacecraft Thermal Control," M.S. Thesis, Univ. of Colorado, Boulder, CO, Dec. 2012.

[2] Nabity, J.A., Holquist, J.B. and Klaus, D.M. (2017), Freezable Single-loop Thermal Control Architecture Assessment and Potential Key Enabling Technologies, ICES-2017-243, 47th International Conference on Environmental Systems, July 2017

[3] Quinn, G., Stieber, J., Sheth R. and Ahlstrom, T. (2015), "Phase Change Material Heat Sink for an ISS Flight Experiment," 45th International Conference on Environmental Systems, ICES-2015-167

[4] Bergman, T. L., Lavine, A. S., Incropera, F.P., and Dewitt D.P., Fundamentals of Heat and Mass Transfer, 7th ed., John Wiley & Sons, Inc.

[5] Nabity, J., Holquist, J., Milanese, M., Lotto, M., and Klaus, D. (2016), Effect of gravity on ice-layer growth in a freezable heat exchanger, Journal of Thermophysics and Heat Transfer, 30(3), 499-512.

[6] Nabity, J. A. (2014), "Modeling a Freezable Water-Based Heat Exchanger for Use in Spacecraft Thermal Control," Journal of Thermophysics and Heat Transfer, 28(4), 708–716. doi:10.2514/1.T4351

[7] BOEING, Dow Active Thermal Control System (ACTS) Overview. https://www.nasa.gov/pdf/473486main_iss_atcs_overview.pdf

[8] Gilpin, R. R. (1981), "Ice Formation in a Pipe Containing Flows in the Transition and Turbulent Regimes," Journal of Heat Transfer, Vol. 103, No. 2, May 1981, pp. 363–368. doi:10.1115/1.3244467.

[9] R. Conde, M.T. Parra, F. Castro, J.M. Villafruela, M.A. Rodrıguez, C. Mendez (2004), Numerical model for two-phase solidification problem in a pipe, vol. 24, 2004, pp. 2501-2509.

[10] MSC. Basic Course of Thermo-Fluid Analysis. http://www.cradle-cfd.com/tec/column01/008.html

[11]Kumano, H., Asaoka, T., Saito, A., Okawa, S. (2009), "Formulation of the latent heat of fusion of ice in aqueous solution," International Journal of Refrigeration, Volume 32, Issue 1, January 2009, Pages 175–182.

[12]Gilmore, D.G., "Satellite Thermal Control Handbook", The Aerospace Corporation Press, 1994.

[13]Weigand, H. Beer (1993a), Freezing in turbulent flow inside tubes and channels, Warme- und Stoffubertragung, vol. 28, 1993, pp. 57-

[14]Weigand, H. Beer (1993b), Ice-formation phenomena for water flow inside a cooled parallel plate channel: an experimental and theoretical investigation of wavy ice layers, International Journal of Heat and Mass Transfer, vol. 36, 1993, pp. 685-693.

[15]Hirata, T., and Ishihara, M. (1985), "Freeze-Off Conditions of a Pipe Containing a Flow of Water," International Journal of Heat and Mass Transfer, Vol. 28, No. 2, 1985, pp. 331–337. doi:10.1016/0017-9310(85)90066-3

[16]Nabity, J. A., Mason, G. R., Copeland, R. J., Libberton, K. A., Trevino, L. A., Stephan, R. A., and Paul, H. L. (2007), "Space Suit Radiator Performance in Lunar and Mars Environments," International Conference on Environmental Systems, SAE Tech. Paper 2007-01-3275, July 2007. doi:10.4271/2007-01-3275.

[17]Chen, J. Activated Carbon Fiber and textiles.

[18]European Space Agency. Space Engineering & Technology. "Thermal Control". https://m.esa.int/Our_Activities/Space_Engineering_Technology/Thermal_Control

[19]ANSYS, Inc. (2009), ANSYS Fluent 12.0 User's Guide.

[20]Nabity, J., Spatafore, B., Mason, G., Hecht, J., Klaus, D. M., and Ewert, M. K. (2013), "A Self-Regulating Freezable Heat Exchanger for Use in Spacecraft Thermal Control," AIAA Paper 2013-3418, 2013.

[21]Nabity, J., Copeland, R., Mason, G., Libberton, K., Paul, H., Trevino, L., and Stephan, R. (2006), "Performance Testing of an Advanced Lightweight Freezable Radiator," International Conference on Environmental Systems, Soc. of Automotive Engineers, Norfolk, VA, July 2006; also ICES Paper 2006-01-2232.

[22]Wang, X., Niu, J., Li, Y., Wang, X., Chen, B., Zeng, R., Song, O., and Zhang, Y. (2007), "Flow and Heat Transfer Behaviors of Phase Change Material Slurries in a Horizontal Circular Tube," International Journal of Heat and Mass Transfer, Vol. 50, Nos. 13–14, 2007, pp. 2480–2491. doi:10.1016/j.ijheatmasstransfer.2006.12.024

[23]Bylander, L. (2010), Spacecraft Thermal Control, Dept. of Space and Plasma Physics, Royal Institute of Technology, Stockholm, 2010.

[24]Leimkuehler, T. A., Stephan, R. A., and Hawkins-Reynolds, E. (2011), "Testing and Failure Mechanisms of Ice Phase Change Material Heat Exchangers," AIAA Paper 2011-5207, 2011.

[25]Leimkuehler, T. O., and Stephan, R. A. (2012), "Experimental Investigation of Ice Phase Change Material Heat Exchangers," AIAA Paper 2012-3520, 2012.

[26]Fukusako, S., and Yamada, M. (1993), "Recent Advances in Research on Water-Freezing and Ice-Melting Problems," Experimental Thermal and Fluid Science, Vol. 6, No. 1, 1993, pp. 90–105. doi:10.1016/0894-1777(93)90044-J

[27]Sankararaj, S. Properties of Fluids. http://mechteacher.com/properties-of-fluids/

[28]Ye, C. and Lin, C. (2006), Numerical Modeling of Solids Precipitation of a Binary ,Mixture Flowing in a Horizontal Pipeline, 9th AIAA/ASME Joint Thermophysics and Heat Transfer Conference, 2006.

[29]Harding, P. (2013), “ISS suffers external coolant loop issue – contingency spacewalks planned,” NASA\\\Spaceflight.com, Dec 11, 2013. https://www.nasaspaceflight.com/2013/12/iss-suffers coolant-loop-issuespacewalks-possible/ [retrieved 2/27/2017]

[30]Copeland, R. J., Mason, G., and Weislogel, M. (1999), “A Freeze Tolerant Radiator,” NASA CR-9-99014, June 1999

[31]Dow Chemical Company, Dow Propylene Glycol, Technical Grade. http://www.dow.com/propyleneglycol/

[32]Eckart, P. (1996), Spacecraft Life Support and Biospherics, Microcosm Press and Kluwer Academic, Norwell, MA, 1996, p. 92.

[33]Comsol. Comsol blog. CFD application. https://www.comsol.com/blogs

[34]Cognata, T. J., Leimkuehler, T., Balasubramaniam, R., Nayagam, V., Hasan, M., and Stephan, R. (2011), “A Review of the Experimental and Modeling Development of a Water Phase Change Heat Exchanger for Future Exploration Support Vehicles,” AIAA Paper 2011-5208, 2011.

[35]Frank M. White, Fluid Mechanics, McGraw-Hill Book Company, 1979

[36]Weast, R., Lide, D., Astle, M., and Beyer, W., CRC Handbook of Chemistry and Physics, 70th ed., CRC Press, Inc., Boca Raton, FL 1990, pp. B-225, D-173-174, D-177, E-6, E-12, F-10, F-37.

[37]Avallone, E. A., and Baumeister, T., III., Marks’ Standard Handbook for Mechanical Engineers, 9th ed., McGraw–Hill, New York, 1987, pp. 19–25.

[38]Smallwood, I. M. (1996), Handbook of Organic Solvent Properties, John Wiley & Sons, Inc., New York, 1996, p. 113.